1956

# The Low Temperature Hall Effect in Single Crystals of Beryllium and Zinc.

Harold William Hemstreet Jr
*Louisiana State University and Agricultural & Mechanical College*

# THE LOW TEMPERATURE HALL EFFECT IN SINGLE CRYSTALS OF BERYLLIUM AND ZINC

A Dissertation

Submitted to the Graduate Faculty of the
Louisiana State University and
Agricultural and Mechanical College
in partial fulfillment of the
requirements for the degree of
Doctor of Philosophy

in

The Department of Physics

by
Harold William Hemstreet, Jr.
B.S., Loyola University, 1950
M.S., Louisiana State University, 1952
August, 1956

ACKNOWLEDGMENT

The author wishes to express his deep appreciation to Dr. Joseph M. Reynolds who supervised this work. He would like also to give sincere thanks to the other members of the low temperature group, in particular Mr. Theodore Leinhardt and Mr. Dennis Triantos, for their cooperation and help. Finally the author must mention his gratefulness to Mr. Charles Burlo who gave much of his extra time in the construction and repair of the glass apparatus.

TABLE OF CONTENTS

# LIST OF TABLES

# LIST OF FIGURES

## ABSTRACT

An introductory discussion of the Hall effect is given, including a resumé of the modifications through which the theory has gone from its inception to the present. The recent observations of field dependent periodic oscillations in the low temperature Hall coefficients of bismuth, graphite, and antimony are cited as the motivation for this work on beryllium at three crystallographic orientations and zinc at one. Detailed descriptions are given of the crystal growing method and the construction of the furnace and molds used. The Hall potential measuring circuitry is discussed. It incorporates several new variations to reduce extraneous potentials and decrease the error spread in the Hall data. The results are given in terms of a new coefficient characteristic of the Hall effect. They reveal no oscillations in the zinc specimen, nor in two of the three beryllium specimens. The results on the third beryllium crystal show uncertain aperiodic oscillations in the reciprocal of the magnetic field. Comparison of these results is made with another recent investigation of the low temperature Hall effect in zinc and beryllium.

# CHAPTER I

## INTRODUCTION

In 1890 E. H. Hall first observed the galvanomagnetic effect that bears his name. It was found that when an electrical current is sent along one axis of a conductor in the shape of a parallelopiped, and that when a magnetic field is present along a second axis perpendicular to the first, there will be a transverse electric field set up along the third axis mutually perpendicular to the other two. This transverse electric field can be measured in terms of the voltage drop across the width of the conductor in that direction.

The Hall effect occurs in more than one form, but the present work will be concerned only with the simplest, namely, the "isothermal dc Hall effect". As its name infers, it is generated with a direct current in a conductor maintained free of temperature gradients.

One can explain the occurance of the transverse voltage drop, the Hall voltage, at least qualitatively in terms of a free electron gas moving through a box. In Fig. 1 electrons are moving upward with velocity $v_y$ under the influence of a downward electric field $E_y$. If the box is subjected to a magnetic field $H_z$ perpendicular to its front and back faces, the electron gas will acquire a velocity component to the left in accordance with the Lorentz force equation.

$$\vec{F} = -e\left[\vec{E}_y + \frac{1}{c}\vec{v}_y \times \vec{H}_z\right]$$

As the electrons accumulate on the left face of the box they will eventually set up a field $E_x$ which nullifies the effect

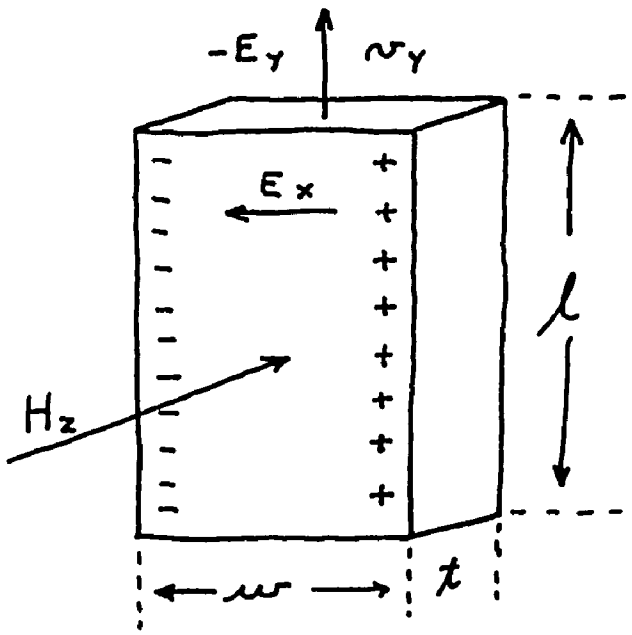


FIG. 1

of the magnetic field, after which time a steady state will exist. The magnetic component of the Lorentz force must be be equal and opposite to the force caused by the transverse electric field $E_x$, that is, their vector sum is zero.

$$-e\vec{E}_x - \frac{e}{c}\vec{v}_y \times \vec{H}_z = 0 \qquad (1)$$

or

$$-e\vec{E}_x = \frac{e}{c}\vec{v}_y \times \vec{H}_z \qquad (1a)$$

If 'N' is the number of electrons per unit volume, then the current density, $\vec{j}_y$ is

$$\vec{j}_y = N e \vec{v}_y \tag{2}$$

and

$$\frac{\vec{j}_y}{N} = e \vec{v}_y \tag{2a}$$

By substituting this last into Eq. 1a there results

$$- e \vec{E}_x = \frac{\vec{j}_y \times \vec{H}_z}{N c} \tag{3}$$

or

$$\vec{E}_x = \left( - \frac{1}{Nec} \right) \vec{j}_y \times \vec{H}_z \tag{3a}$$

It is seen from this last equation that for a given 'N' the value of the Hall field, $E_x$, depends only on $j_y$ and $H_z$. The ratio $E_x/j_y H_z$, called the Hall coefficient and designated by R, serves as an index of the relative size of the Hall effect in a given conductor. When measuring R one usually expresses it in more directly accessible parameters by the following transformation:

$$R = \frac{E_x}{j_y H_z} = \frac{V_x / w}{I / w t} \cdot \frac{1}{H_z} = \frac{V_x t}{I H_z} \tag{4}$$

where 'I' is the total current through the conductor in the y-direction, and 'w' and 't' are its width and thickness respectively, and $V_x$ is the Hall voltage.

The simple free electron treatment presented above predicts that the Hall coefficient should be equal to -1/Nec, as can be seen from Eq. 3a. Surprisingly enough the observed values especially in the monovalent metals agree to a fair

approximation with the predicted values. It will be noted that the theory presupposes a Maxwell-Boltzmann distribution of electron energies, which is far from being the case. If the theory is modified by applying Fermi-Dirac statistics to the electron gas, the agreement between observed and calculated values is not greatly improved. Because of the negative sign of the electronic charge these theories always give a negative sign to the calculated coefficient; is positive. This more serious conflict can be resolved, at least qualitatively, by assuming that the carriers involved in the Hall process have effectively a positive charge. Another alternative is to assume that 'N', the number of electrons per unit volume, can be considered a negative number, which is to say that the electrons involved behave effectively as though they had negative mass. It is believed at present that either viewpoint is correct. In fact the theory as it is now set up implies that both concepts are merely two different ways of saying the same thing.

In the foregoing model of an electron gas one might want to include the interaction of the electrons with each other. This gives at most a negligible improvement of the picture, and it obviously does not explain the occurance of a positive coefficient. The more modern theories of the transport phenomena in a conductor use the quantum mechanical

approach and take into account the fact that the electron is moving through a periodic lattice and undergoes interactions with it. This treatment gives rise to what is known as the band theory of solids or the band approximation. It has given a clear, yet relatively simple, explanation of the hitherto anomalous positive Hall coefficient.

A brief word of introduction to the foundations of the band theory might be worth mentioning here. If one considers, for example, an electron drifting through a crystal lattice. it is seen that it undergoes periodic changes in its potential energy as it passes near the lattice centers. The electron is moving in a sea of three dimensional wells, the periodicity of the wells being that of the lattice, and the depth and shape of the wells also being characteristic of the particular crystal and its lattice. Since the electron is no longer free, but must be considered partially bound, its "free electron" wave function,

$$\psi = e^{i\vec{k}\cdot\vec{r}}$$

must be modified according to the binding potential. Bloch[1] has shown that the new wave functions have the form

$$\psi = u_k(\vec{r})\, e^{i\vec{k}\cdot\vec{r}} \qquad (5)$$

where the function $u_k(r)$ is periodic with the periodicity of the lattice. The exact form of the function $u_k(r)$ depends on the degree of binding of the electron to the atom. It ranges from zero everywhere when the electron is perfectly free, to a constant in the immediate vicinity of a free

atom and zero elsewhere (the case of an inner shell electron). The chief concern here is with the intermediate case where the potential energy of the electron is neither free nor a localized constant, but varies periodically. The energy of a free electron is a continuous function of its momentum and hence of its wave number vector k; that is,

$$E(\vec{k}) = \frac{\hbar^2}{2m} \vec{k}^2 \qquad (6)$$

If k is confined to $k_x$, the above equation gives a plane parabola; in any case it puts no restriction on the energy but allows all values. At the other extreme, where the electron is tightly bound to the inner shell of a free atom, its energy is sharply limited to discrete values, all others in between being forbidden. However, in the intermediate case of the electron partially free in the lattice, it turns out that the energy spectrum is characterized by continuous bands of allowed energy separated by gaps of forbidden energies. Hence when the wave functions for electrons have the form of Bloch functions (Eg. 5) no solutions of the wave function exist for certain ranges of energies. The energy parabola may then be considered as being distorted by finite discontinuities as shown in Fig. 2 (one-dimensional case).

From Eq. 6 the second partial derivative of energy with respect to wave number is

$$\frac{\partial^2 E(k)}{\partial k^2} = \frac{\hbar^2}{m}$$

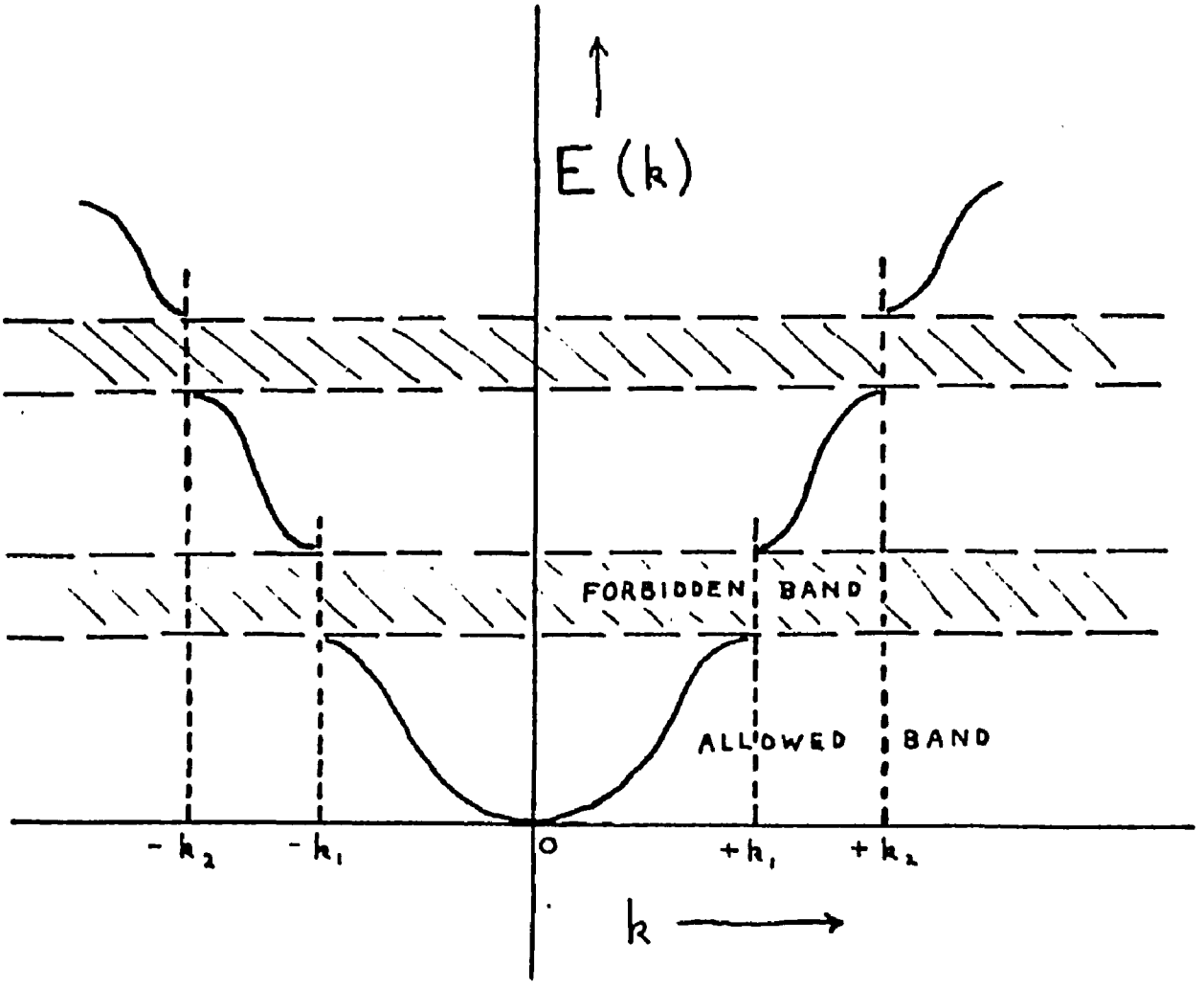


Fig. 2 The Energy Parabola

and

$$m = \hbar \left( 1 \Big/ \frac{\partial^2 E(k)}{\partial k^2} \right). \qquad (7)$$

For a smooth parabola the second derivative is of course everywhere constant and Eq. 7 gives the rest mass of the electron provided relativity effects are neglected. Let the mass be deinfed by Eq. 7 and written as

$$m^* \equiv \hbar \left( 1 \Big/ \frac{\partial^2 E(k)}{\partial k^2} \right) \qquad (7a)$$

It will be seen that for situations in which the electron is not perfectly free, and in particular for the situation depicted by the broken parabola of Fig. 2, m* (called the effective mass) will in general be different from the rest mass. Its value will depend on the location of the electron in its energy spectrum. If it has, for instance, an energy near the top of an allowed band, the second derivative in Eq. 7a, on this portion of the broken graph, is negative; therefore the effective mass as defined above is also negative.

In two-dimensional k-space the points on the k-axis of Fig. 2 representing forbidden energies become lines in the $k_x$-$k_y$ plane. These lines form regular polyhedra centered about the origin and serve to partition the space into what are called Brillouin zones. The extension to three dimensions merely gives a series of closed surfaces of ever

increasing size but all centered at the origin. It often happens in both the two and three dimensional representations that successive polyhedra intersect one another at certain regions in the k-space, that is, the zones may overlap for certain directions. The shape and size of the zones depend only on the structure of the crystal lattice.

The electrons in a metal, say at 0° K, do not all have zero energy, nor any other single energy because of the exclusion principle. The well known Fermi-Dirac distribution function, which is based on the principle, predicts for electrons and certain other particles a uniform energy distribution from zero to some maximum. This function places a rigid restriction on the occupancy of the energy levels rather than on the electrons themselves, that is, it allows each level a specific number of occupants depending on the degeneracy. Since electrons are completely indistinguishable in this scheme, no such restriction is binding on them; they may in time take on various energies in the Fermi-Dirac spectrum provided they do so by exchanging with other electrons. The criterion is that the statistical energy balance must be maintained.

As the temperature of the metal is raised above absolute zero the highest filled energy level, the Fermi level, and the few immediately below begin losing their occupants to higher levels which were formerly empty. All the lower lying levels in general remain undisturbed.

In terms of the band approximation one then could consider a given solid as being characterized by a particular Brillouin structure with the Fermi level lying in one of the zones (in three dimensions the level becomes an energy surface). The position of the Fermi level in the zone pattern determines to a great extent the transport properties of the solid. If for example the level lies close to the inner edge of a zone, that is, near the bottom of an allowed band, the electrons occupying this top level are readily able to assume higher energies under applied forces. Thus an external electric field would easily upset the statistical balance by accelerating these few top level electrons to higher energies. This would be in a given direction and cause a net velocity opposite the field (for negative charges) different from zero. On the other hand a solid whose Fermi level lies just inside a zone boundry, hence just below a forbidden band, will not have its statistical balance so easily disturbed by an external field. None of the electrons including the upper level ones can be accelerated to the levels just above because these levels lie in a forbidden band. All the allowed levels below the forbidden band are filled so that no change is possible unless the upper level electrons are given sufficient energies to jump the forbidden gap into the next allowed band. The solid in this latter case would be an electrical insulator, whereas in the former case it would be a conductor. Considering the anomalous or positive Hall effect one sees that

this takes place in those solids whose Fermi level lies in the upper portion of an allowed band where the effective electronic masses are negative. The transport phenomena in such solids occur as if the energy were transmitted by positively charged carriers. Such carriers are called holes. The outline of the band theory presented above omits many of the details and ramifications growing out of the theory. It is meant to give at most a qualitative glimpse of the assumptions generally used in treating the Hall effect and other conduction phenomena.

In 1954 the Hall effect in bismuth at liquid helium temperatures[2,3] was investigated in this laboratory. The Hall coefficient had the negative sign but showed an oscillatory dependence on magnetic field, being periodic in the reciprocal of the field. The period was independent of temperature but its amplitude decreased with increasing temperature and all but disappeared above 4° K. Actually the oscillations were superimposed on a monotonic term that was concave upward. Closely following this work the oscillatory Hall effect was found at low temperatures in graphite[4] and antimony.[5] This behavior in bismuth and the others is not wholly unexpected in view of the related behavior of the field dependent magnetic susceptibility and magnetoresistance, and of the more recently discovered thermal conductivity and thermoelectric power effects. The first such field dependent oscillations were found by de Haas and van Alphen in

the magnetic susceptibility of bismuth at liquid hydrogen temperatures in 1930.[6] Unsuccessful attempts were made to observe the effect in other metals. In the meantime Peierls[7] developed a theory based on a simple cubic lattice showing that oscillations should be expected. Blackman[8] and Landau[9] using the rhombahedral lattice of bismuth further extended the theory. It was not until 1947 that the effect was observed in a second metal, when at this time Marcus[10] detected it in zinc. Since then numerous workers, notably Shoenberg[11] and Berlincourt,[12] have established the presence of the "de Haas - van Alphen effect" in a host of other metals at low temperatures.

The second such field dependent periodic effect was established in bismuth in 1953 when Alers and Webber,[13] using magnetic fields up to 100 kilogauss, observed definite oscillations in the magnetoresistance as a function of field. The oscillations like those of the susceptibility were periodic in 1/H. A short time later Berlincourt made measurements on the susceptibility of the same bismuth crystal, which confirmed the propinquity of the two effects.

In regard to the Hall effect it must be said that as long ago as 1940 Gerritsen and de Haas[14] observed an anomalous behavior in bismuth. Their graph of Hall coefficient versus magnetic field showed several large irregular maxima and minima which do not correspond to the recent results obtained in this and other laboratories [2,3,15]. The former results are believed to be erroneous since they are at variance

with the present Hall data as well as the susceptibility and magnetoresistance data of bismuth, all of which are in substantial agreement. Shortly after the observance of oscillations in the Hall coefficient of bismuth, Steele and Babiskin[16,17] found a similar field dependent periodicity in the thermoelectric power and the thermal conductivity of bismuth.

An equation for the periodic Hall coefficient in bismuth has been derived by Grimsal and Levinger[18] based on the Peierls, Blackman, Landau theory for the de Haas - van Alphen oscillations. The basis of the formulation is the fact that the electrons (carriers) responsible for all the aforementioned effects are relatively small in number, and that this number changes periodically with reciprocal magnetic field. Thus the quantity 'N' occuring in the classical equation

$$\vec{E}_x = \left(-\frac{1}{Nec}\right) \vec{j}_y \times \vec{H}_z \qquad (3a)$$

must be replaced by a periodic function.

Dingle[19] derived the quantity

$$N = N_0 + \sum_{p=1}^{\infty} \frac{(-1)^p}{p^{3/2}} \frac{m^{3/2}}{2\pi^3\hbar^3} \frac{p\chi}{\sinh p\chi} (\beta^* H)^{3/2} \sin\left(2\pi p \frac{E_0}{\beta^* H} - \frac{\pi}{4}\right) \qquad (8)$$

for the number of electrons per unit volume giving rise to the de Haas - van Alphen effect, where

$$\chi = \frac{2\pi^2 k T}{\beta^* H}$$

$E_0$ is the Fermi surface energy, and $\beta^*$ is an effective double Bohr magneton given by

$$\beta^* = \frac{e\hbar}{m^* c}$$

Grimsal and Levinger derived by a different method the same equation for N. Before applying it to the calculation of the Hall coefficient they simplified it somewhat by assuming that at low temperature and high fields ($2\pi^2 kT \ll \beta^* H$) $\chi$ was small enough so that the hyperbolic sine could be replaced by

$$\exp\left(-2\pi^2 kT/\beta^* H\right)$$

They further simplified it by dropping all but the first term of the summation, which in effect limits the oscillations to a single period, a result that is correct for only one orientation of bismuth. With these two approximations N becomes

$$N = N_0 - \frac{m^{3/2}}{\pi\hbar^2} kT \exp\left(-\frac{2\pi^2 kT}{\beta^* H}\right)(\beta^* H)^{1/2} \sin\left(2\pi\frac{E_0}{\beta^* H} - \frac{\pi}{4}\right) \qquad (9)$$

In defining the effective mass above (Eq. 7a) it was tacitly assumed that k referred to one direction only. It is readily seen that in a real anisotropic lattice m* becomes a tensor, which has its simplest form in a cubic lattice. One must therefore know the shape of the surfaces of constant energy in k-space in order to construct a universal model for transport phenomena. The present lack of such information for all but the simple lattice structures leaves a dis-

turbing gap in the general theory. Grimsal and Levinger used the isotrpic (sperical energy surfaces) two band model in their treatment, where in the first band

$$E = \frac{\hbar^2}{2m} \alpha_1 \vec{k}^2 \tag{10}$$

and in the second or inverted band

$$E = A - \frac{\hbar^2}{2m} \alpha_2 \vec{k}^2 \tag{11}$$

The quantity A is the energy width of a forbidden band, and the $\alpha$'s are equal to $m/m^*$, where $m^*$ is an average effective mass in k-space for each band. This is the simplest model which allows for both positive and negative Hall coefficients. The resulting isotropic two band Hall effect formula, after slight modification, is

$$R \cong -\frac{1}{ec} \frac{N_1 \alpha_1^2 - N_2 \alpha_2^2}{(N_1 \alpha_1)^2} \tag{12}$$

Putting Eq. 9 into this formula they get an expression for the Hall coefficient of the form

$$R = R_0 - R_1 H^{1/2} T \exp\left[-\frac{2\pi^2 kT}{\beta^* H}\right] \sin\left(\frac{2\pi E_0}{\beta^* H} - \frac{\pi}{4}\right) \tag{13}$$

where $R_0$ and $R_1$ are constants. Eq. 13 seems to agree semi-quantitatively with the oscillatory part of the experimental results, but it does not predict the field dependence of the non-oscillatory part that is observed experimentally.

The present work was undertaken in an attempt to detect the oscillatory Hall effect in other metals. It seemed most reasonable to explore metals that had already shown de Haas - van Alphen oscillations. Beryllium was selected first because, in addition to satisfying the above requirement, its lattice structure (hcp) is not too complex and its room temperature Hall coefficient is reasonably large compared to the other de Haas-van Alphen metals that had not already been investigated. The second choice was zinc because, despite its small room temperature Hall coefficient, it was the second metal to show the de Haas-van Alphen effect. It also has the hexagonal close packed lattice.

In 1950 and 1952 Borovik[20] also investigated the low temperature Hall effect in beryllium and zinc. Copies of his articles, which were in Russian, were obtained and translated by one of the members of this laboratory. Borovik's results showed no oscillations, nor was he searching for them at the time; rather he was interested in pointing out the primary dependence of the Hall coefficient R on the magnetoresistance of a given crystal. It is customary to characterize the Hall effect by the coefficient R as defined in Eq. 4, and this yields a most reliable index of the Hall process. However, as Borovik shows, for situations in which the resistance of a sample increases with magnetic field (as it does in the case of bismuth at helium temperatures to an enormous degree) this coefficient

is influenced by the change in resistance so that it is no longer a measure solely of the Hall effect. In place of R he suggests the use of the quantity $E_x/E_y$ as being more representative, where $E_x$ is the Hall field and $E_y$ the field due to the working current through the sample. This ratio might be expected to be a true Hall constant practically independent of magnetic field. However, Borovik's results on Be, Zn, and Al show that it is not, which of course is to be anticipated in view of the recent Hall theories outlined above and the present low temperature data on bismuth, graphite, etc.

Following his suggestion a similar departure was made in the present work from the traditional methods of plotting Hall effect data. Another coefficient was devised which was easier to compute from the data of this research than either Borovik's ratio or the ordinary coefficient R, and which retained his central idea in that it was independent of the magnetoresistance. This will be discussed in more detail in the last chapter.

## CHAPTER II

## PREPARATION OF SINGLE CRYSTALS

The Crystal Furnace. Previous to the present work the author had constructed a furnace specifically for the growing of single crystals by the Bridgman method.[21] Since the furnace had been successful in producing large single crystals of bismuth and antimony, it was again utilized, along with the techniques already developed, in the preparation of the zinc specimens.

The furnace was in the form of a hollow thick walled cylinder open at both ends. Fig. 3 shows several views without the accessories and stand. The inner wall consisted of two half-cylinder alundum forms; the inside surface of these cylinders was indented with circular bores running the length of the cylinder and parallel to the axis. These are conventional manufactured forms designed for the construction of electric furnaces. No. 20 Nichrome wire wound into long helical springs served as the heater elements. Sixteen such springs were wound on the lathe and all cut to the same length of about 15", slightly longer than the bores in the alundum forms. They were inserted into the holes, eight in each half-cylinder, and connected together as follows: The eight elements in one half-cylinder were connected end to end in series, as were the eight in the other; both groups

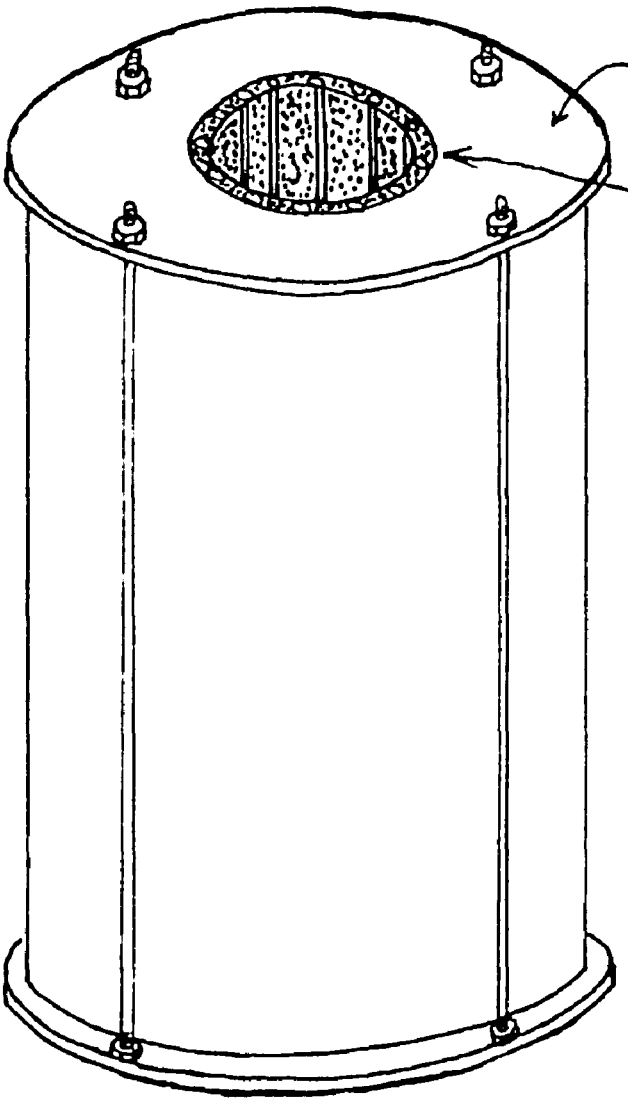


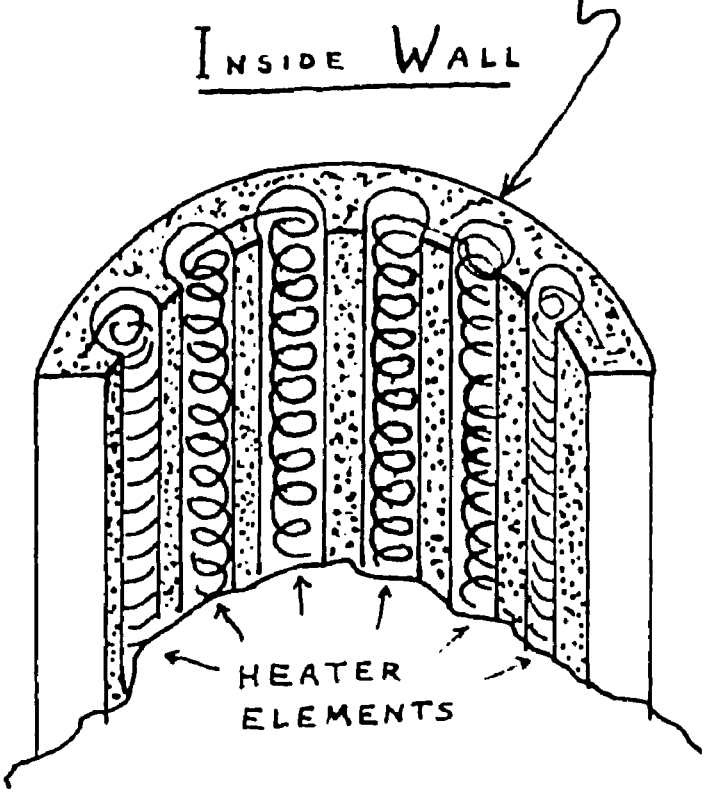


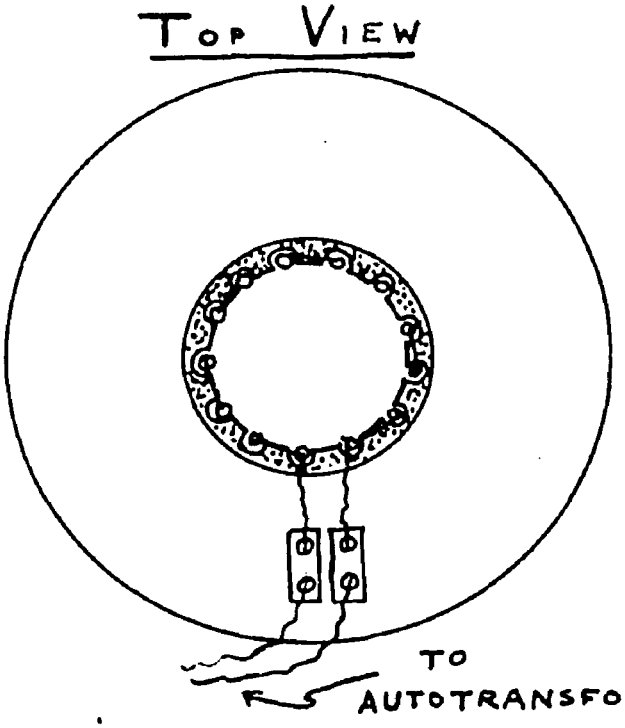


Fig.3 Body of Furnace

of eight were then connected together in parallel. The final arrangement is partially illustrated in the cut-away view in Fig. 3. Since the individual elements had a room temperature resistance of approximately 3 ohms, each group of eight in series had a total resistance of 24 ohms, giving an overall resistance for the heater of 12 ohms.

The two half-cylinders were bound together by several extra pieces of Nichrome wire to form the complete cylinder. Each end of the cylinder was inserted snugly into the center holes, cut for the purpose, of a pair of flat circular discs made of asbestos board. These discs were 1/4 inch thick with an outer diameter of 13 inches and an inner diameter of 2-1/2 inches (the outer diameter of the alundum cylinder). A circular groove 12 inches in diameter and concentric with the inner hole was cut on one side of each disc; then a section of galvanized sheet iron was rolled into a right circular cylinder 12 inches in diameter so that each end could be inserted into the grooves on the asbestos discs. The above components were assembled as shown in Fig. 4, but before adding the cover the inner space between the heater element forms and the outer wall of the furnace was filled with firmly packed alundum powder. Four equally spaced 3/16 inch holes were drilled around the outer rim of both the upper and lower covers, and when the upper was put on it was bolted to the lower by means of four end threaded steel rods running the length of the furnace out-

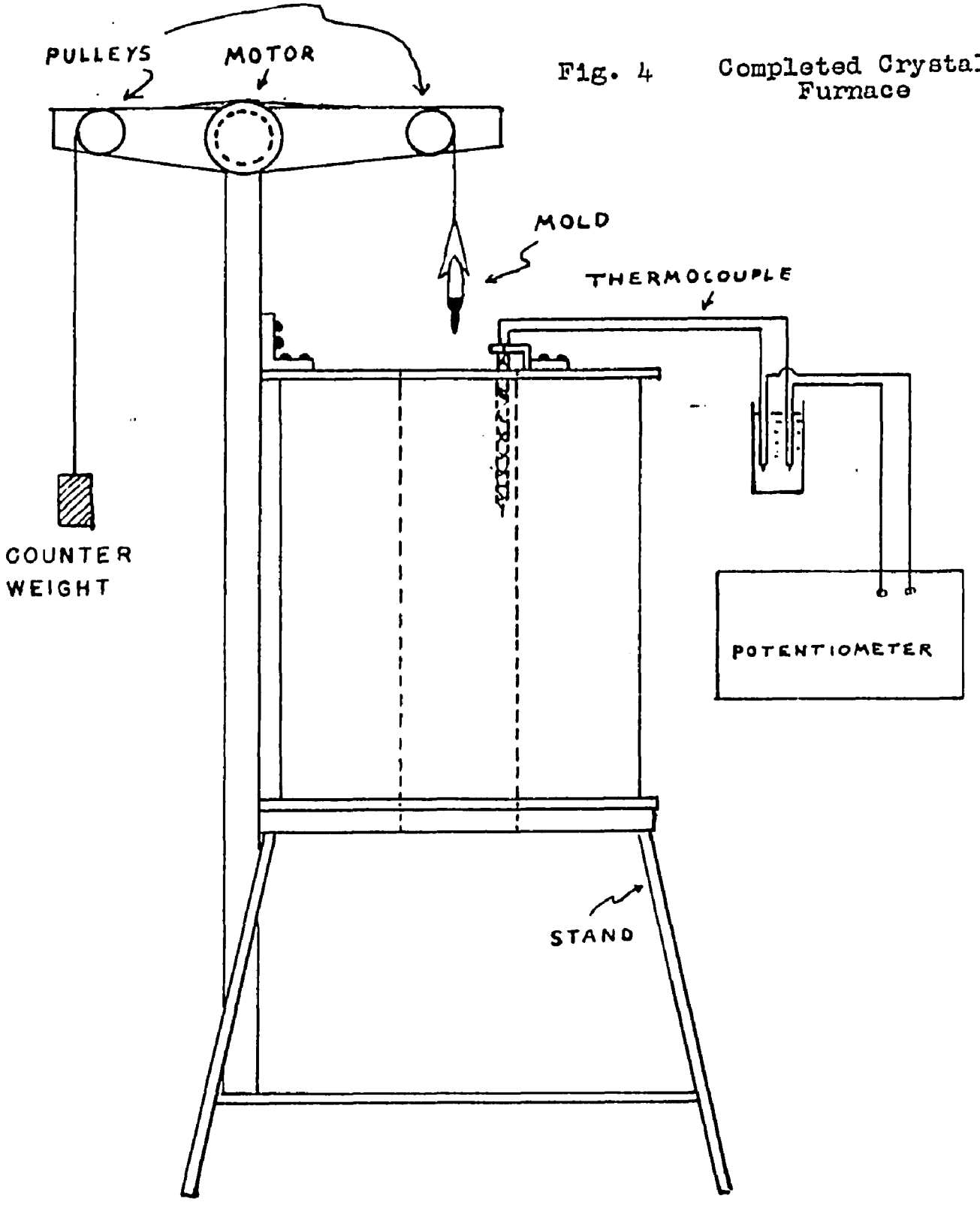


Fig. 4 Completed Crystal Furnace

side of its outer wall. This completed the body of the furnace.

The base of the furnace consisted of a four-legged metal stool with a large hole cut in the seat. It was bolted to the bottom cover so that its hole lay directly below the furnace opening, allowing a clear passage through the furnace to the floor.

A synchronous clock motor was mounted 14-3/4 inches above the top of the furnace opening in the center of a brass cross-arm. The motor was not directly above the opening but off to the side about 6 inches so that its shaft was in a plane tangent to the outer wall. At each end of the cross-arm was an aluminum pulley 1 inch in diameter. These two pulleys were identical, each having a square groove cut around its edge and being free to turn about an axis parallel to the motor shaft. The motor shaft turned at the rate of 1/12 of a revolution per hour. A third aluminum wheeel larger than the other two was fastened to the motor shaft. This system of motors and pulleys was situated so that the outer edge of one of the small wheels was directly above the center of the furnace opening, and the outer edge of the other small wheel was several inches beyond the outside wall. As Fig. 4 shows the crystal mold was suspended from one end of a thin flexible steel cable which had a counter weight at the other end. The center of the cable was looped twice around the center

driving wheel and then passed over the top and side of each of the free turning wheels. When the motor was started the mold descended slowly through the furnace, the rate of descent being determined by the circumference of the driving wheel. It was found that a rate of about 2 cm. per hour gave satisfactory results, so the driver was made with a circumference of 23.5 cm.

The Crystal Molds. Zinc melts at a temperature of 420° C. This is not too far below the softening point of pyrex glass (about 550° C), so under ordinary conditions it might be considered unwise to grow a zinc crystal in a pyrex mold. Quartz glass would suggest itself because of its high melting temperature. However, the molds were made of pyrex instead of quartz for reasons that will be given later.

Fig. 5 shows views of the completed mold. Section A was approximately 3" long with a hollow rectangular cross section; B and C were 6" and 3" long respectively with hollow circular cross sections. These latter were made from stock pyrex tubing and separated by a slight "seal off" constriction. The construction of section A was more involved. A flat rectangular mandrel was milled from a piece of hard steel to a thickness of a little under 1/16 inches. All surfaces were further ground and polished by hand to a mirror finish; at the same time a slight taper from one end to the other was introduced. The taper was so small as to

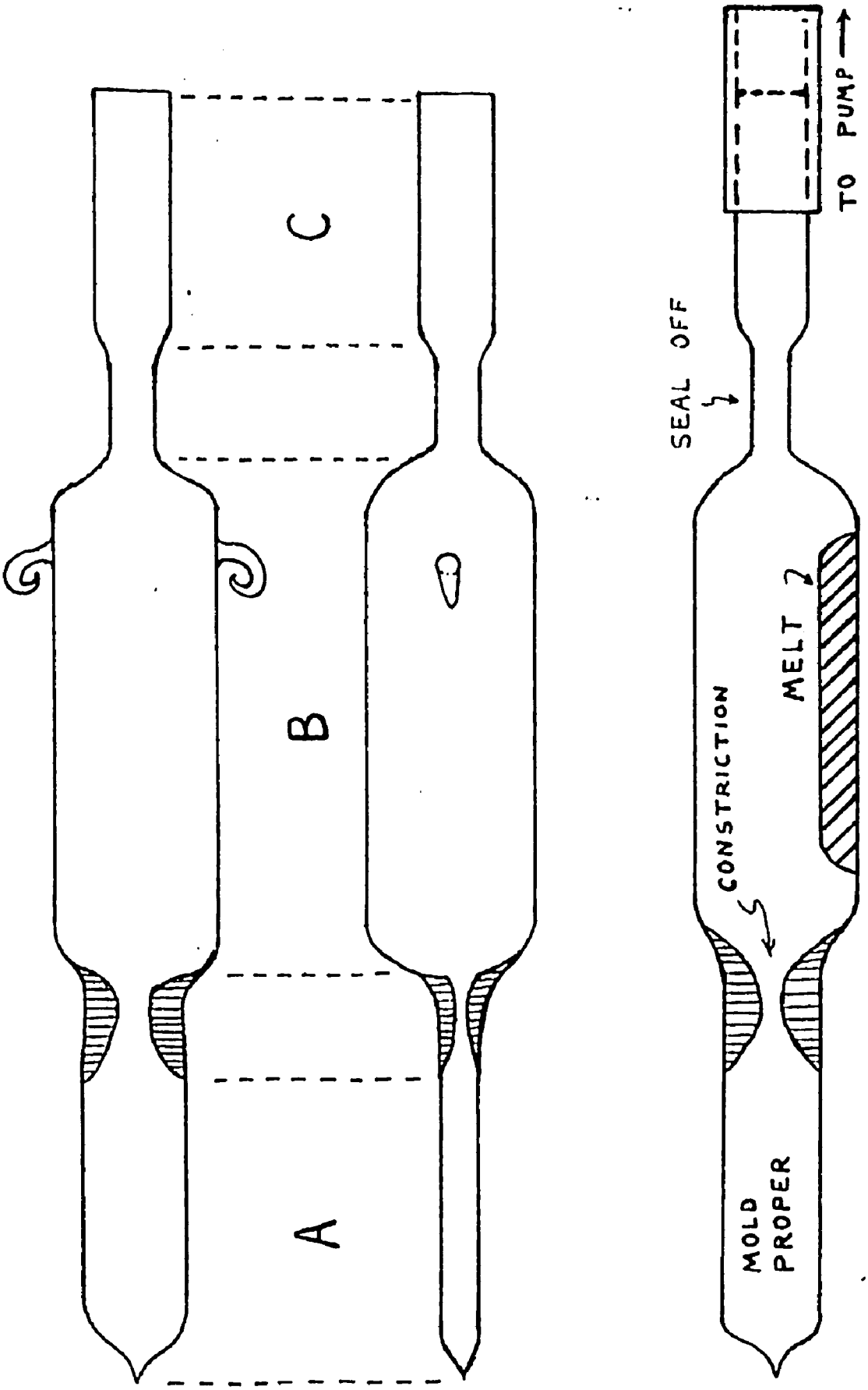


Fig. 5 The Crystal Mold

be unnoticeable except by actual measurement. The dimensions of the mandrel, 3-/2" x 3/8" x 1/16", were not critical but the uniformity and flatness of the faces were.

Next a length of stock pyrex tubing about 2 feet long was heated uniformly over a 10 inch section near its center until soft. This section was placed between two pieces of asbestos board and pressed together. The object was to flatten the tube and leave just enough space between the walls to allow the mandrel to be inserted after the glass cooled. To accomplish this with some degree of control, spacers were held between the board to prevent them from collapsing the glass too far. Of course the original diameter of the tube was chosen so that the width as well as the collapsed section was only slightly greater than that of the mandrel. One end of the flattened portion was cut off for inserting the mandrel. Before doing this the mandrel was coated with a layer of carbon black. This was done by dipping it in carbon tetrachloride and then exposing all surfaces to the tip of a candle flame. It was then inserted into the flat section. The glass was heated to the softening point and allowed to collapse completely onto the mandrel. After cooling, the glass was cut off at the wide end of the mandrel so that it could be pulled out. The carbon served as a satisfactory lubricant, but much of it remained on the inside walls and corners of the glass. Most of this residue could be washed or scaped out; the remainder had to

be burned out by waving the glass rapidly through a medium hot flame.

It was mentioned earlier that pyrex was used in preference to quartz in spite of the former's relatively low softening point. If the quartz had been used it is believed that the high temperature required to collapse it around the mandrel would have warped the steel.

One end of Section A in Fig. 5 was closed by drawing it to a fine point. This point was to house the seed which started the crystal growth. Its exact size and shape was unimportant. Past experience with several shapes and sizes indicated that all had about the same efficacy for seeding a crystal. The other end was joined to Section B through the heavy walled capillary as shown. B and C were connected by the seal-off constriction, and the other end of C was left open for connection to a vacuum pump. Two solid glass hooks were attached to opposite sides of B close to the constriction.

The insides of the mold were thoroughly cleaned before using. A rubber suction bulb was attached to the open end of C to suck different cleaning solutions into the mold through the other end (the seeding tip was left open for this operation and later closed). The procedure followed here was similar to that used in cleaning glass surfaces for silvering. First, concentrated nitric acid was sucked up to the top of the mold, then it was shaken moderately for

a short time and squeezed out. Next followed several rinses with distilled water. The above procedure was repeated with the following solutions: concentrated potassium hydroxide, a 5% solution of hydrofluoric acid, and distilled water containing a few drops of ammonium hydroxide in that order. The distilled water rinse was included between each solution, and several were given after the last.

Growth of the Crystals. The zinc was purchased from Jarrell-Ash Co. (Newtonville, Mass.) in the form of spectroscopic rods (JM 15Q). Its purity was given as 99.999 per cent. An estimate was made of the volume of zinc necessary to fill Section A of the mold, and this amount was broken off from the rods. The pieces were etched in dilute nitric acid enough to remove all surface oxides and placed in Section B of the mold. To do this the glass had to be cut apart 1/2 inch below the hooks on B and sealed together again after insertion. The mold was clamped in a horizontal position to a stand and connected to a fore vacuum pump and allowed to evacuate. After a few minutes a gas-air torch was applied along the length of the mold in a back and forth motion to heat it uniformly. It was usually necessary to have on hand a second torch, this one gas-oxygen, to melt the metal and keep it in the molten state while the other one kept the rest of the mold hot. At this stage the melt had begun to outgas and the process was speeded by tapping on the mold or its stand at a regular frequency. Extreme care had to be taken so as not to over-

heat the glass while keeping the zinc molten.

Along with the adsorbed gas molecules, other impurities were released from the metal; because a crust gradually formed and floated on the surface of the melt during outgassing. Studies on crystal structure and impurities indicate that much of the impurity content of a polycrystal resides in the crystallite boundries; and when a crystal is grown from the melt the bulk of the impurities move along with the advancing interface that separates the solid from the melt. Before melting the zinc it was seen from the etch pattern that it consisted of crystallites whose average volume was of the order of 3 cubic mm., while the total volume put into the mold was of the order of $10^3$ cubic mm. These magnitudes point to a relatively large total area for the boundary surfaces of the crystallites. Presumably the loose crust on the surface of the melt was formed largely of impurities released from the disintegrating boundary layers.

When the outgassing stopped the melt was gradually poured from B to A by tipping the mold into a vertical position. The capillary obstructed a large percentage of the surface crust. With the mold in a vertical position and Section A filled, it was ready to be sealed off and suspended in the furnace. However, at this stage it was found that a few stationary bubbles had collected in the melt, probably as a result of delayed outgassing. They were worked out by tapping and the constriction between B and C

was sealed off. The remainder of the mold (A and B) was unclamped and inserted halfway into the furnace. It was held in the furnace to prevent the zinc from solidifying while the mold was being fastened to its suspension cable above. The cable had two loops on the end and these were slipped over the glass hooks on the mold. Finally the motor was started and the mold began its descent.

The center of the furnace was maintained at a temperature of approximately 470° C, which was 50° above the melting point of zinc. An iron-constantin thermocouple was used to measure the temperature. Its hot junction was placed close to the center of the furnace but not too close to obstruct the passage of the mold.

About 20 hours after starting the motor the bottom section of the mold had usually dropped completely through the furnace. The mold was removed and Section A was cut off at the constriction. It was placed in a paraffin trough of concentrated HF and allowed to set until the glass had dissolved. The zinc crystal was etched lightly in dilute $HNO_3$ or $H_2SO_4$. By observing the etch pattern of metal crystals one can determine whether or not they are singular. The surface of a polycrystal will be divided into a number of irregularly shaped areas, each of which will reflect the maximum light at a different angle. Because of this the areas are distinctly observable. In this way it was determined whether a single crystal or a polycrystal had been grown. The specimen was considered useable when it consisted

of one large crystallite; or when several crystallites were formed and one was large enough to be cut into a flat rectangle of suitable dimensions. The cutting was done on a glass cutting saw (a water-cooled carbarundum wheel) by holding the specimen firmly clamped between two pieces of lantern slide glass and letting the saw slice through the glass as well as the zinc. In the first place this method enabled the operator to keep a strong grip on the zinc with little danger of twinning or bending it; secondly, it prevented the trimmed edges of the crystal from becoming frayed during the cutting.

The method outlined above produced about one near perfect single crystal for every four grown, and of the three that were not singular one usually contained a large crystallite which could be cut to size and used. Thus useable specimens were produced practically 50 per cent of the time. The most serious deficiency inherent in the method was that it could not provide for orienting a crystal, that is, there was no way of seeding the crystal or forcing it to grow with its crystallographic axes aligned in a prescribed direction relative to the geometric axes of the mold. Hence the principal crystal axis always made a skew angle with the principal geometric axis.

Determination of Orientation. The crystallographic orientation of the zinc crystal (Zn-1) was determined with an optical goniometer. It was found that the best etch pattern in zinc for use with the goniometer was produced

by a dilute sulphuric acid solution. The error in determining the orientation was fairly large because the collimated light pencil was diffused to some extent after reflection from the principal crystallographic planes. The measurement showed that the hexagonal axis (c-axis) made a skew angle of $24 \pm 3°$ with the geometric axis that was perpendicular to the large face of the crystal. Hence in the Hall measurements the hexagonal axis made an angle of approximately 24° with the magnetic field.

The beryllium single crystals were not grown in this laboratory but were purchased from Nuclear Metals, Inc. (Cambridge, Mass.) Three flat rectangular crystals were ordered. All were roughly the same size, but each had a different orientation of its crystal axes relative to its geometric axes. Their size and orientations are given in Table I below.

Table I

Dimensions and Orientations of Crystals

| | | | |
|---|---|---|---|
| | a-axis | - | c-axis |
| Be-1 | 1.275 cm. | 0.806 cm. | 0.103 cm. |
| | a-axis | c-axis | - |
| Be-2 | 1.285 cm. | 0.784 cm. | 0.152 cm. |
| | c-axis | - | a-axis |
| Be-3 | 1.362 cm. | 0.851 cm. | 0.294 cm. |
| | - | - | - |
| Zn-1 | 1.370 cm. | 0.866 cm. | 0.086 cm. |

Upon receipt of the crystals from the company it was found that two of them were too large to fit the crystal

holder used for the Hall measurements. Rather than construct a larger holder the top and sides of the oversize crystals were trimmed on the carbarundum wheel. The dimensions given in the table are those of the specimens after trimming.

## CHAPTER III

## MEASURING APPARATUS AND INSTRUMENTS

The crystal whose Hall effect was to be measured was suspended in a bath of liquid helium inside a double set of pyrex Dewar flasks. The flasks were mounted so that their bottom sections (where the crystal was located) hung between the pole faces of a large electromagnet, and the crystal was always situated with its flat faces perpendicular to the magnetic field. Four copper leads extended through separate holes in the helium flask cap down into the bath and connected to the crystal. The other ends went to the measuring instruments. In barest outline this was the arrangement for making the low temperature Hall measurements.

The magnet used throughout the experiments was a Weiss type electromagnet built by Mr. T. E. Leinhardt of this laboratory. The pole faces were 4 inches diameter and spaced 1-5/16 inches apart. At this spacing it was estimated that the field intensity diminished by not more than 1 per cent from the center to the outside edges of the faces. The overall error in measuring the field was about 100 gauss.

The Flask Assembly. Two pyrex glass Dewar flasks were part of the apparatus. One held liquid nitrogen at room pressure, the other held liquid helium under pressures

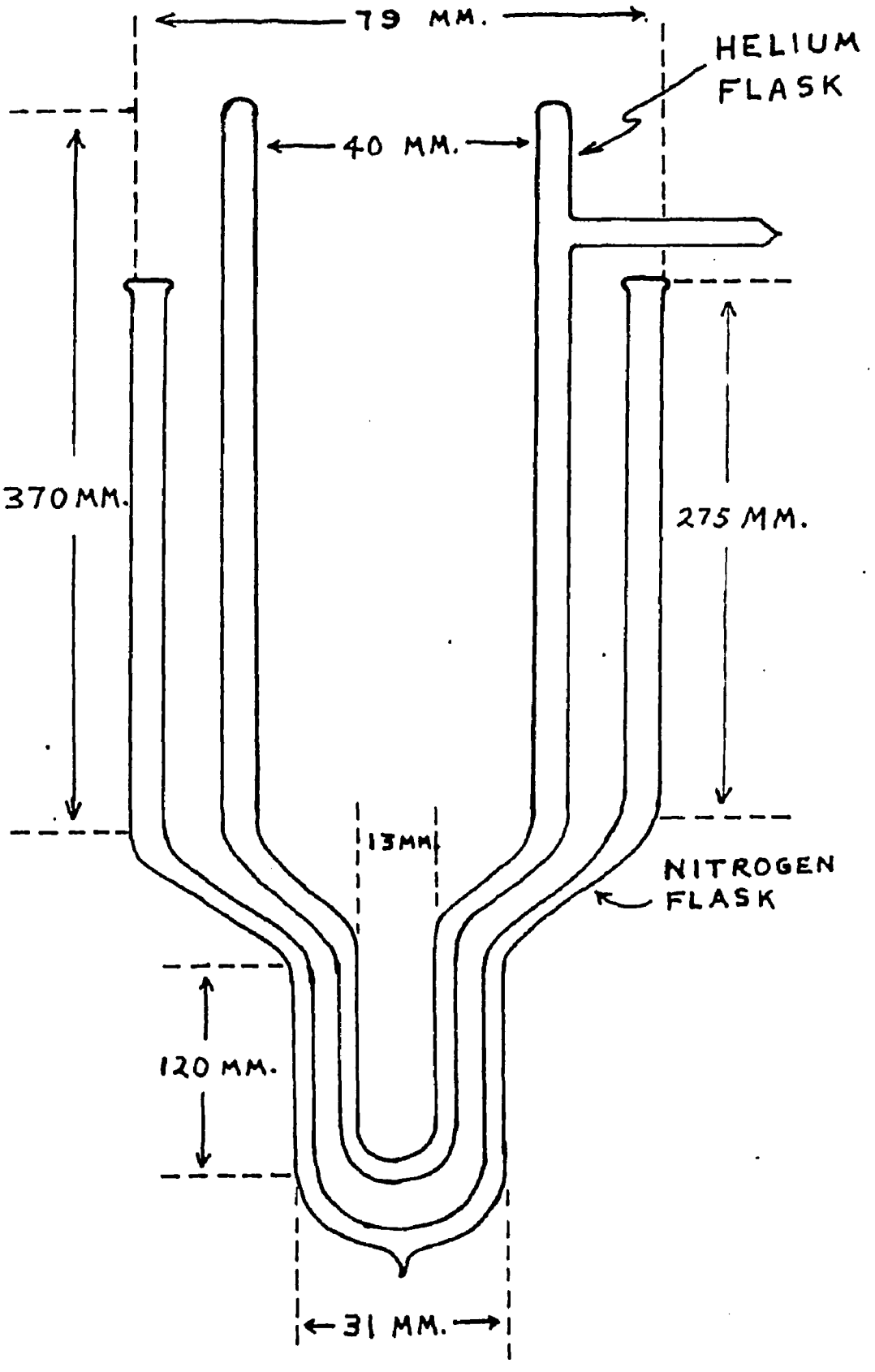


Fig. 6 The Flasks

ranging from 1mm. of Hg to room pressure. The helium flask was immersed in the nitrogen flask as shown in Fig. 6. Both narrowed down to a smaller diameter at their lower ends, which hung in the space between the magnet pole faces. The flasks were silvered, but a 1/2 inch wide unsilvered vertical strip was left on opposite sides of each one. It was possible to align all four strips and view the inside of the inner flask from either side. The space between the walls of the nitrogen flask was pumped down to a hard vacuum and permanently sealed off at the bottom. In the case of the helium flask it was not possible to evacuate and seal it off permanently. Pyrex glass is porous to helium gas at room temperature; thus a vacauum in the inner space could not be expected to last. It was necessary to pull a vacuum of only 2 or 3 mm. of Hg because when the flask was filled with liquid helium the small amount of air in the inner space would freeze and leave a sufficiently hard vacuum. However, this flask had to be evacuated after each use because of its porosity to warm helium.

To hold the crystal in place in the bottom of the helium flask and in its proper position in the magnetic field a Lucite holder was constructed. A piece of Lucite stock was turned on the lathe to a diameter of 0.51 inches so that it could slide easily into the lower section of the helium flask. It was cut to a length of 1-1/4 inches. Next a deep slot was milled in one side to a depth of half its diameter and 7/8 inches long (see Fig. 7). Two additional

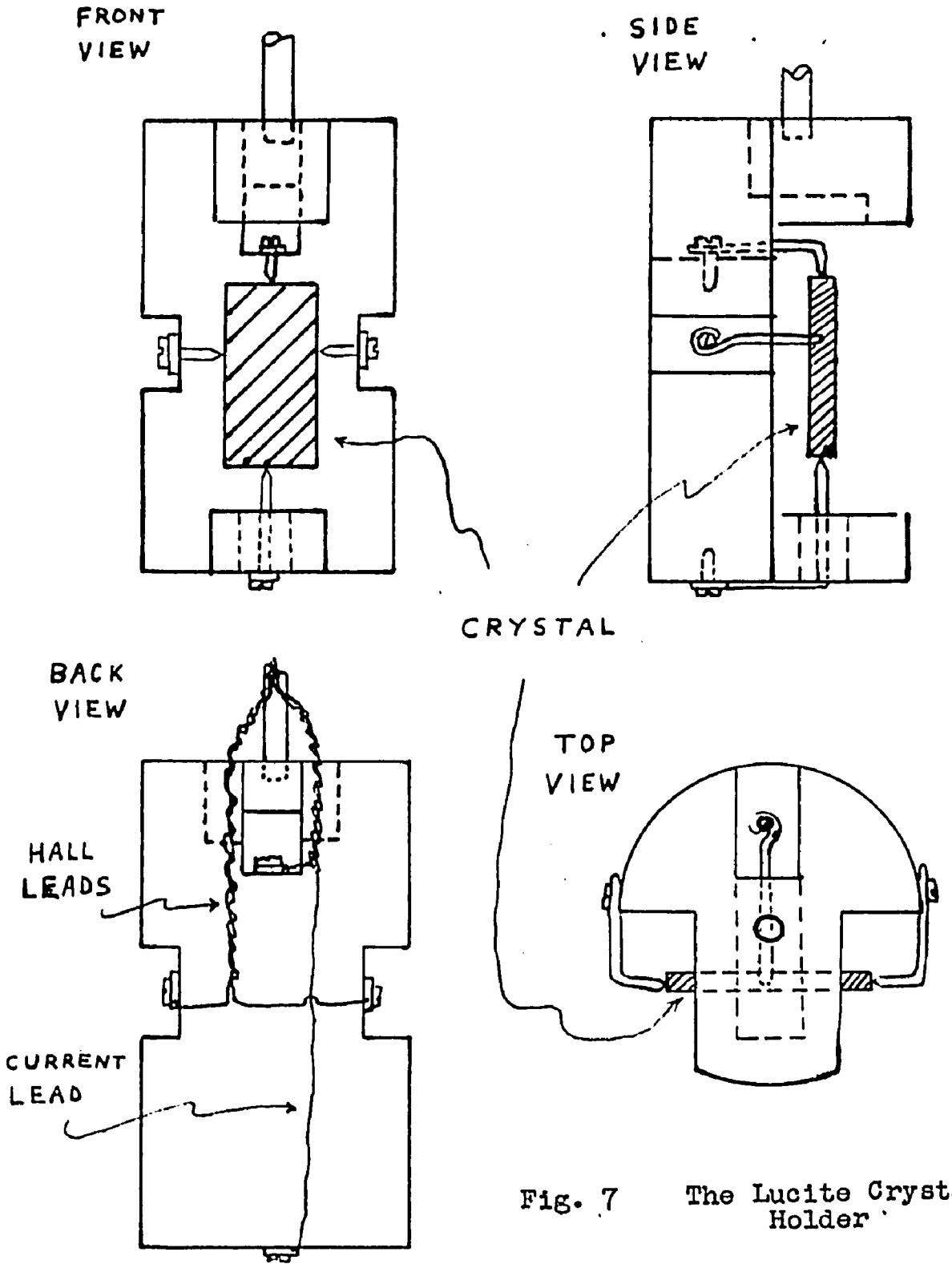


Fig. 7 The Lucite Crystal Holder

but smaller slots were cut into each side of the rod (in this description the large slot is taken as the front of the rod) so that they were perpendicular to the first one. Two 90° pie wedges were cut from the top lid on either side of its front half and two more from the bottom lid as illustrated in the "Top View" of Fig. 7. These latter openings allowed free passage to helium bubbles that formed beneath the holder during an experiment. Five slots were cut lengthwise along the back surface to allow additional space for the passage of bubbles. Next a rectangular block was cut from the back top corner. It extended down below the thickness of the top lid 1/8 inch and into the lid less than halfway. The bottom part of this opening was further extended by cutting a square opening into the large front slot at its top corner. Thus there was a sizable opening joining the front and back sections of the holder. A short hole was drilled in the top center of the Lucite and another one through the bottom lid halfway between center and front. Finally four small tapped holes were drilled in the following places: one each in the two side slots, one in the bottom lid off center toward the back, and one in the bottom of the indentation in the upper back section. The holes were so placed that the top and bottom ones were coaxial, as were the two side ones; and the axes were coplanar and perpendicular.

Four hooked probes made of phosphor bronze were held in place by the screws that fitted the tapped holes. The probes had two important functions: primarily, they made the electrical contact to the crystal, secondly, they held the crystal rigidly in place. There was nothing else touching the crystal except the temperature bath. The tips of these probes were filed to a round sharp point.

The crystal holder was suspended from a long slender Lucite rod which was cemented into the hole at the top of the holder. The other end of this rod was cemented to the underside of the flask cap. Several views of the cap are shown in Figs. 8 and 9.

With the exception of the copper manometer tube, which was silver soldered into the hole as shown, the cap was made in one piece from brass stock. Its central vertical tube connected to a rubber vacuum hose which in turn was connected to a high capacity vacuum pump. It also served as the orifice through which the filling spout from the helium liquifier was inserted. Adjacent to this tube and arranged in a semicircle were the four holes through which the electrical leads were brought into the flask. Only one of the holes is shown in the diagrams of Figs. 8 and 9, and it will be noticed that the top halves are flared. The sides of the cap which overlap the flask were threaded from the bottom to halfway up; then right above the threads was attached a circular clamp with an arm extending out from each side. These arms rested on two additional parallel

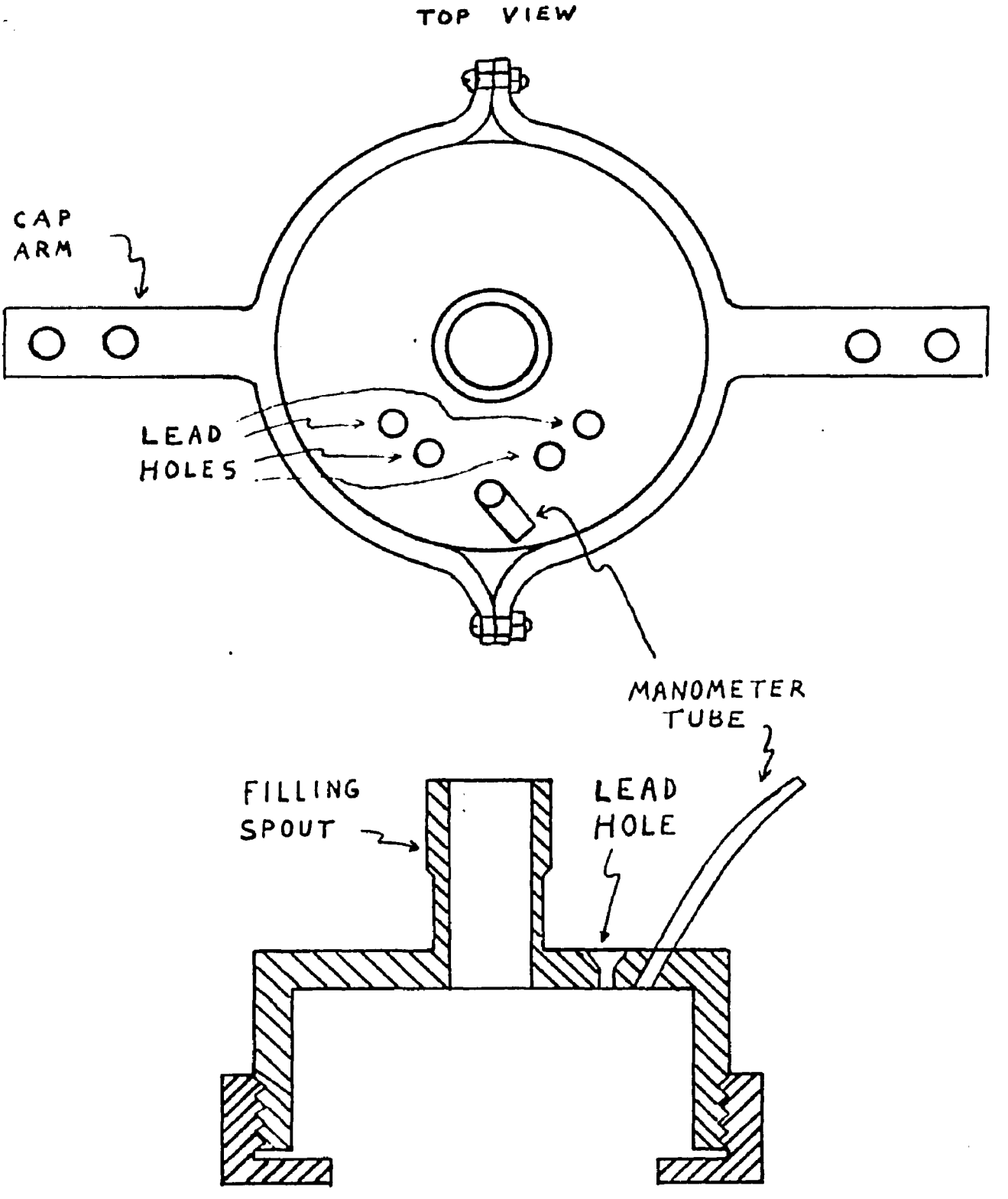


Fig. 8 The Flask Cap

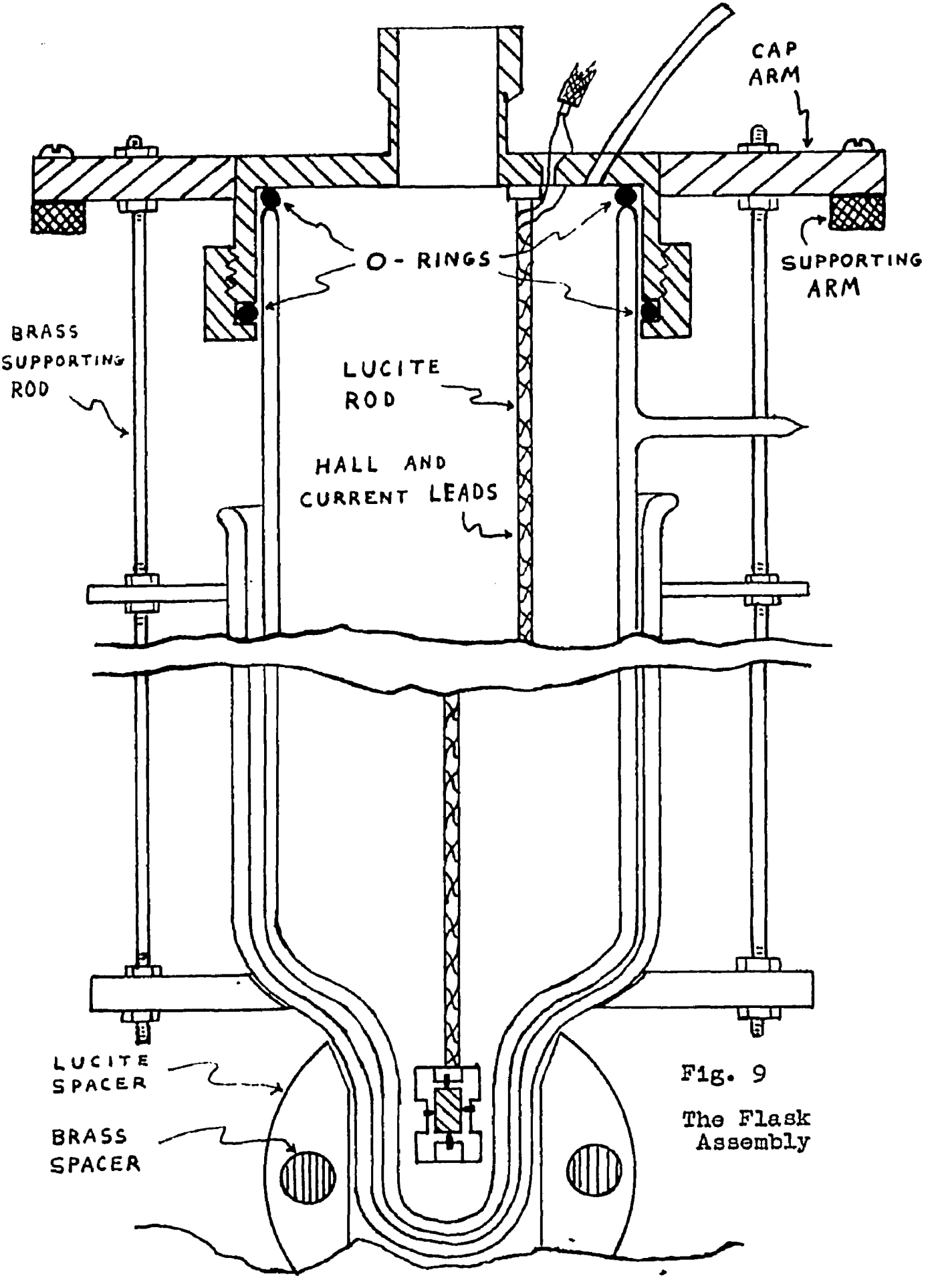


Fig. 9

The Flask Assembly

arms which were part of a rigid frame attached to the magnet (end view shown in Fig. 9).

The cap rested on an O-ring placed on top of the flask. It was the purpose of this O-ring to act as a cushion between the metal and glass. A second O-ring stretched around the flask was pushed up until it made firm and uniform contact with the lower edge of the cap. An inside threaded ring with a bottom lip extending almost to the flask walls was screwed up onto the cap. The edge of the cap in contact with the O-ring was beveled upward toward the inside, so that as the metal ring was screwed tight the O-ring was squeezed against the flask and the cap. A light coat of silicon stop cock grease was spread on the O-ring before each use. The same brand of grease was used on all the hose and tube connections of the vacuum system.

The outer flask was suspended from the cap arms by means of two long rods and two Lucite supports. One of these had a hole through its center, so that it slipped over the bottom and up against the shoulders of the flask. The other had a larger hole enabling it to slip over the body of the flask and up against the lip at the top. The rods extended from a hole in each cap arm down through holes on each side of the Lucite supports. Hence both flasks and the crystal were all suspended from the cap, which itself was fastened to the metal frame on the magnet.

Since the width of the air gap between the pole faces of the magnet was adjustable, two brass cylinders 1-5/16 inches long were used as spacers to maintain this specific separation between faces. The spacers were embedded in a

large Lucite cylinder whose height was exactly that of the spacers and whose diameter was that of the pole faces. A hole was cut completely through the side of the Lucite along one of its diameters so that it passed between the spacers. The cylinder and spacers were lodged between the pole faces with the hole vertical; and the bottom of the outer flask fit snugly into the hole, thus aligning the lower portion of the flask in the field.

The Measuring Circuit. The circuit used for the Hall measurements consisted essentially of the following units: a Rubicon Microvolt Potentiometer, Cat. No. 2786 (Rubicon Co., Philadelphia, 32, Pa.), a Liston-Becker DC Breaker Amplifier, Model 14 (Liston-Becker Instrument Co., Inc., Stamford, Conn.), a Leeds & Northrup Type K Potentiometer, a box galvanometer, a 0.1 ohm standard resistance, and a voltmeter (1000 ohms/volt).

It was anticipated that the Hall coefficients in beryllium and zinc at liquid helium temperatures would be extremely small, and that the Hall voltages encountered would be fractions of a microvolt. This required the measuring circuit to have high sensitivity and especially to be free of extraneous emf's. These emf's usually encountered are the ac pickups, contact potentials, thermal emf's (Seebeck and Thomson effects), and the voltages induced by a double ground.

Fig. 10 shows the complete circuit, which can be subdivided into the current circuit for measuring the working

current through the sample, and the Hall circuit for measuring the voltages on the Hall probes. The first employs the standard potentiometric technique for measuring current accurately. The ammeter shown in the circuit diagram was used to give a continuous approximate reading of the current. All three batteries were conventional 6 volt storage batteries, and each one supplied a specific circuit, that is, the different cells of one battery were not used in different circuits. If only one cell was required to supply current, as for the Type K Potentiometer, the other two were unused.

In the Hall circuit the null indicating device was a combination dc amplifier and voltmeter instead of the usual galvanometer. Since the smallest scale division on the Rubicon Potentiometer was 0.005 microvolt (interpolation was possible to 0.001 microvolt), the sensitivity had to be comparably high. A galvanometer of such sensitivity must be mounted and adjusted with extreme care and is highly susceptible to minute room vibrations. The method employed here is to amplify the unbalance of the potentiometer with a dc breaker amplifier and feed the output to a relatively insensitive voltmeter. This method is sound provided the drift and background noise of the amplifier are not excessive. Previous experience with the present amplifier showed that the noise was negligible, and the drift though present was not too serious. It was estimated that the amplifier enabled the potentiometer to measure 1 microvolt with an accuracy of 1 part in 250.

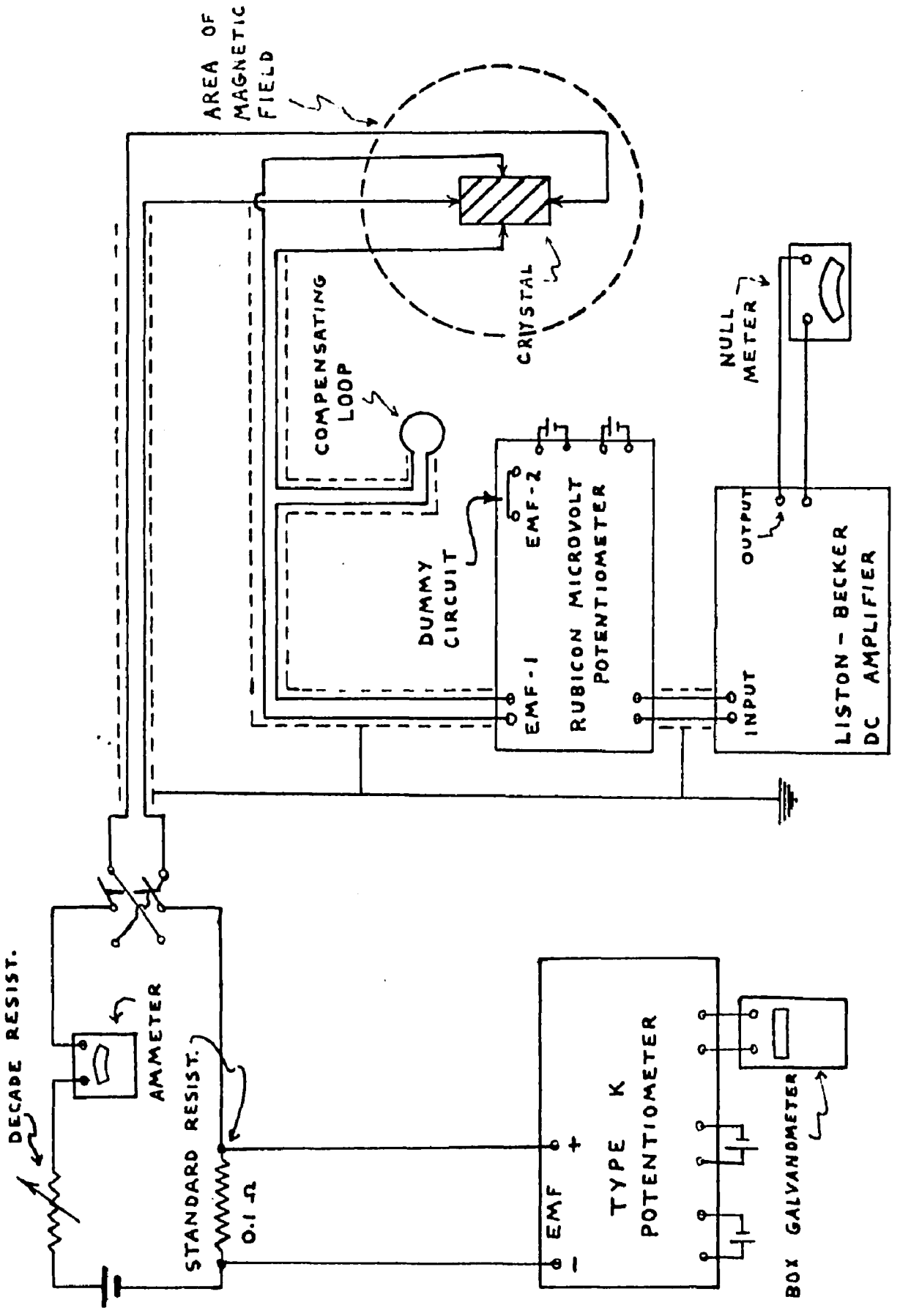


Fig. 10 The Measuring Circuit

As mentioned earlier the circuit had to be designed almost free from extraneous emf's. To eliminate the ac pickup, potentiometer and amplifier were both shielded by their metal enclosures. The Hall and current leads also had to be shielded especially in view of their exposed length, which was about 8 inches apiece.

In cryogenic work requiring the use of electrical leads inside the cryostat, it is standard practice to select very small wires for the purpose. This is done to minimize the rate of heat flow into the cryostat via thermal conduction. For this reason the Hall leads were made of No. 32 wire, which is small yet strong enough to be handled repeatedly without breaking. The current leads were made of larger wire, No. 26, in order to safely carry the large sample current (1.5 to 2.0 amperes).

Reference to the crystal holder diagrams of Fig. 7 will show how the Hall and current leads were soldered to their respective probes, then brought over and around the back of the sample holder, and finally up along the Lucite rod to the holes in the cap. In particular it will be noticed that these pairs of leads connected to the sample present small open loops to the magnetic field, which is perpendicular to the place of the "Front- and "Back View" diagrams. The slightest ripple or change in the field would induce emf's in the circuit too large to be tolerated. To overcome this deficiency a compensating loop was included in series in the Hall circuit (see Fig. 10). This loop, which was actually

part of one of the Hall leads, was wound around a Lucite disc of 3/4 inch diameter and placed opposite the magnet air gap so that it looped the flux just outside the pole faces. It was fastened to a horizontal Lucite rod which pointed toward the air gap. The rod was clamped in a friction bushing so that it could turn about its long axis. Thus the amount of stray flux threading the loop was adjustable from zero to a maximum in either direction. The loop was adjusted to make the emf induced in it equal and opposite to the total emf induced in that part of the Hall circuit between the pole faces. There was no need for such a device in the current circuit.

Both sets of leads were twisted together, but each pair was kept separate from the other. After trying different methods of twisting the leads without breaking or kinking them, the simplest and safest procedure was to clamp the two ends of a pair in the bit of a hand drill then clamp another point of the pair (some distance from the ends) between two pieces of cork held in a vise. The length between the drill and the vise was twisted slowly and not too tightly to prevent the insulation from being scraped off. The remaining sections had to be twisted together beneath the flask cap after they were strung through the separate cap holes. After twisting, each set was covered with "spaghetti" then with a braided shielding cable along the entire sections that were to lie outside the flask. The lengths inside were twisted but left uncovered. Each of the

four leads entered the flask through individual holes in the cap. The holes were then filled with a sealing wax. Care was taken to keep the wires centered in their holes to guard against the possibility of electrical shorts developing between the wires and the cap.

Below the cap the two pairs were wound around the Lucite rod and brought down behind the sample holder as described earlier. They were connected to the probes with a special thermal free solder. These were the only solder junctions in the Hall circuit. The only other connections of any kind were the pressure contacts between the probes and sample and the connections at the EMF binding posts of the Rubicon Potentiometer. These were copper binding posts.

The unbalance at the G. Binding posts of the Rubicon Potentiometer was fed through a shielded cable to the input jack of the dc amplifier. One side of the input was grounded to the chassis and likewise the shield. This shield was connected electrically to those on the Hall and current leads, and all three were grounded by means of a single wire connected to a cold water faucet. Thus the following components were all at the same ground potential: The Hall and current lead shields, the shield on the amplifier input leads, the amplifier chassis, and the Rubicon Potentiometer chassis.

The dc input to the amplifier was chopped by an 8 cycle breaker and the resulting voltage was amplified. At the output the amplified signal was reassembled by a second breaker

which was synchronized with the first. Both were driven by cams on the same motor shaft to achieve perfect synchronization. The input breaker was enclosed in a metal box to prevent dust from getting on the points and to shield it from the rest of the circuit. The input tube and its contiguous components were encased in a shock mounted metal box to shield them and to eliminate microphonics. The amplifier's maximum gain under optimum operating conditions was rated as $10^8$. In the present research the highest gain realized was about $10^7$. There was on the cabinet a set of coarse and fine "Position Control" dials which fed an adjustable dc voltage of either polarity to the input. This voltage was tapped from a voltage divider across a 1.5 volt cell. A 1000 ohm/volt multiple range voltmeter was used at the output as the null indicating meter for the Rubicon Potentiometer. Its lowest range, 0 - 1.5 volts, was used in the experiments, and its pointer was set at half scale by means of the "Position Control." This half scale setting became the zero reading or position of balance for the potentiometer. The amplitude of the background noise at the output in terms of an equivalent signal at the input was well under $10^{-9}$ volts. The overall drift was estimated, again in terms of an equivalent drift signal at the input, to be less than $10^{-8}$ or 0.01 microvolts per hour.

The Rubicon Potentiometer had two sets of emf binding posts labeled "EMF-1" and "EMF-2." The Hall leads were con-

nected to EMF-1 and a copper lead was shorted across EMF-2. This latter "dummy circuit" was certain to be free from the extraneous emf's and other troubles that were found in the Hall circuit; it therefore provided a convenient means of checking the general working order of the circuit and instruments.

# CHAPTER IV

## PROCEDURE

Preliminary Circuit and Apparatus Tests. In getting set up for an experiment the first step was to clean the surface of the crystal to be used by etching it lightly in a dilute acid (nitric for zinc and sulphuric for beryllium). The tips of the phosphor bronze probes were also cleaned by daubing with dilute nitric acid. The crystal was held in position in the Lucite holder while the probes were screwed tightly against it. The two important objects here were to obtain good electrical contact and to align the probes properly, that is, to set the line joining the Hall probe tips perpendicular to and coplanar with that joining the current probe tips. The soundness of the contacts could be checked by measuring the total resistance of the Hall and current circuits. It was known that the Hall circuit had a resistance of 8.5 ohms and the current circuit 1.8 ohms when good contact was being made; any higher readings indicated poor contact. Checking the probe alignment was more difficult. After the first rough visual alignment the leads were connected to the instruments and a sample current sent through the crystal. The magnitude of the voltage measured on the Hall probes indicated the degree of misalignment, and

the polarity of this voltage told its direction. In reality this was an IR drop caused by the probes being on two different electric equipotential surfaces. One of the Hall probes was loosened and moved in the direction necessary to decrease the IR drop, and a measurement was again taken. This trial and error process continued until the IR drop could no longer be diminished. What remained was subtracted out of the Hall data in a way that will be explained later.

The resistance of the leads was again measured with the sample in liquid nitrogen to see if the probes had maintained good contact during the thermal shock. If not, it was necessary to remove the nitrogen, warm and dry the crystal, repair the faulty contact, and then repeat the alignment procedure. If the contacts were good, a trial run was made at the nitrogen temperature. This was done to check the general working order of the instruments and apparatus, but especially to ascertain the order of magnitude of the Hall effect at that temperature before proceeding to the liquid helium temperatures. If the nitrogen trial run was successful, the apparatus was considered working well enough to try the helium run on that crystal.

The measurements made on each crystal at helium temperatures were preceded by preliminary preparations which had become standardized for low temperature experiments at this laboratory. Before assembling the crystal, cap, and flask unit several simple adjustments had to be made to procure proper alignment and positioning of the crystal in the magnetic field. This was done by suspending the cap

from the supporting arms above the air gap allowing the Lucite holder and its crystal to be situated approximately in the center of the gap between pole faces. The supporting arms which held the cap were adjusted up or down until the crystal was centered vertically between the pole faces. Next they were adjusted sidewise and at the same time the cap was rotated slightly until the crystal was centered horizontally and its front and back faces were parallel to the pole faces. The correctness of this latter alignment was determined by sighting through the air gap from each side and from above. There were four threaded holes in each supporting arm and one unthreaded hole at the end of each cap arm. By making the above adjustments in combination the crystal was centered and aligned so that the hole in each cap arm fit over one of the four threaded holes in each supporting arm. Hence, when the crystal assembly was inserted into the flasks and the cap screwed on, the cap cross arms could be placed on the supporting arms in the position of best alignment, as determined by the above process, and held securely by a pair of screws.

During the course of each run the crystal had to be rotated 180° in the magnetic field. This was accomplished by unscrewing the cap arms and rotating the entire cap and flask assembly until the cap arm holes were again above the chosen pair of threaded holes in the supporting arms. As it turned out this rotation proved more awkward than may appear because of the asymmetry of the flasks. The bottom

part of each flask (the narrow portions between the pole faces) was tilted slightly with respect to the main body, so that during rotation this bottom section was turning snugly in the Lucite spacer between the pole faces while the rest of the assembly was precessing about a central axis. This was undesirable and caused difficulty in screwing the cap to the same pair of threaded holes after it was rotated. In spite of this it is estimated that the crystal after rotation was within 2° of the desired 180° position.

The Helium Runs. The helium used in all the experiments was liquified in the laboratory's ADL Collins Helium Liquifier. It normally required four hours to collect enough liquid helium for a given run, and it was during this liquifying period that the flask assembly was flushed out and precooled. The flushing and precooling processes were performed as follows: First, the filling tube on the flask cap was connected to the manifold of the high capacity vacuum pump by means of a large rubber vacuum hose; then the manometer tube on the cap was connected to a "tee," one arm of which went to the mercury manometer and the other to a helium cylinder. With the helium cylinder closed the pump was turned on and the helium flask evacuated. Next, the rubber hose between pump and flask was squeezed together by means of a drill vise especially modified for this purpose; then the helium cylinder was cracked open

letting the gas leak into the helium flask until its pressure returned to atmospheric. The flask was again evacuated and then refilled with helium gas as above. This was repeated three or four times to completely purge the flask of air and leave only a helium atmosphere within. At this point the outer flask was filled with liquid nitrogen in order to precool the flasks and helium atmosphere. As the helium pressure dropped due to the cooling, more gas was leaked in from the cylinder. Actually the pressure was maintained 3 or 4 mm. above room pressure so that any leaks present in the system would let helium out rather than air and other gaseous impurities in. The rate of cooling was relatively slow due to the small amount of exchange gas (about 1 mm. of $H_g$.) between the walls of the helium flask and required an hour or more to complete.

When a sufficient amount of helium had been liquified, the entire flask assembly, including the Hall and current leads, was transferred to the filling tube of the liquifier, filled, and returned to its original position in the magnet. Both sets of leads were checked for continuity to make certain that good contact was maintained with the crystal during the filling of the flask. The leads were then connected to the measuring instruments as previously described (see the circuit diagram, Fig. 10). Next, the compensating loop was mounted in its position adjacent to the Lucite spacer between the magnet poles and adjusted in the following way. The magnet was turned on and its current set at approximately 20 amps., giving a field of 5000 gauss.

It was then turned off, allowing the rapidly decreasing field to induce in the Hall circuit a large emf as seen on the Rubicon Potentiometer. The compensating loop was rotated so as to reduce the net emf generated in the circuit by a changing flux, and this new position was checked by again turning the field on and off. This trial and error procedure had to be repeated many times until the loop was oriented so that its induced emf cancelled that of all other stray loops in the field, that is, until a rapidly changing field produced no deflection in the potentiometer. Complete cancellation was never fully realized in these experiments, however, the induced emf's were reduced to a negligible value especially at low magnetic fields.

Finally, with zero magnetic field and zero current through the crystal, the Hall circuit was checked for extraneous emf's by comparing it to the dummy circuit (the lead shorted across the second pair of emf binding posts on the potentiometer). The procedure was to balance the potentiometer against the standard cell, then center the null indicating meter using the dummy circuit. Presumably there were no extraneous emf's in the dummy circuit, excluding the negligible background noise of the dc amplifier. Hence, this center setting of the null meter was taken as the zero reading of the measuring instruments. Then the Hall circuit was switched in and a potentiometer reading taken. This reading gave the total spurious emf present in

the circuit. When it amounted to less than 0.02 microvolts, the apparatus was considered to be in its best working order; whereas, if the emf was much above this arbitrary value, it indicated the presence of a defect in the circuit serious enough to prevent continuation of the run. One recurrent source of trouble lay in the flask cap where the Hall and current leads passed through the cap holes. It seems that one of the leads would become partially or directly shorted through the sealing wax to the grounded cap. This could be remedied either by "floating" the cap or by pulling the faulty lead away from the cap toward the center of its hole. The latter was the better solution but more precarious, as it required remelting the wax to center the defective lead in its hole. A second common nuisance was the large amount of moisture that condensed on the cap because of the cold vapors below. Apparently the wax was slightly hydroscopic and formed an electrolyte potent enough to form minute batteries in conjunction with the copper leads and the brass cap. The only solution was to keep the cap dry by blowing warm air over it. An ordinary hair dryer proved most effective for this task. Fortunately, it was not necessary to keep the dryer on the cap throughout the entire run, because after the liquid helium level receded some distance below the cap and the liquid itself was brought below the "lambda" point, the condensation became negligible.

The working current sent through the sample was set at some value between 1.5 and 2.0 amperes. Its exact value was measured to four significant figures using the Type K Potentiometer (see circuit diagram). It was monitored continuously throughout the run and its value recorded from time to time, or whenever it changed. Actually the changes were slight, occurring only in the fourth significant figure. An emf reading was taken with the current on but with zero magnetic field to ascertain the IR drop due to the misalignment of probes.

The magnetic field was turned on at its lowest value and the first Hall reading taken; then successive readings were taken as the field was slowly increased in steps up to its maximum value slightly under 14 kilogauss. The field intervals were large at first but were decreased at the higher fields. The reason for taking fewer readings at low fields was to save time. Because of the large current sent through the sample the helium boiled away rapidly, allowing little time to complete without refilling the flask.

After the above described series of data were completed the flasks and sample were rotated 180°. Since now the magnetic field penetrated the crystal in the opposite direction the polarity of the Hall potential was also reversed; hence, the Hall leads at the potentiometer binding posts were reversed. The compensating loop was readjusted for the new position of the crystal, the potentiometer was balanced against the standard cell, and Hall measurements

were again taken from 0 to 14 kilogausss.

This experimental procedure was employed with no essential changes for all four crystals investigated. All measurements were made at the lowest temperature available which was approximately 1.5°K, the exact value varying slightly from one run to another. The large Joule heat dissipated in the current leads by the high current (up to 2 amperes) boiled off the helium much faster than usual. This raised the equilibrium pressure that was obtainable with the vacuum pump operating at full capacity, and hence raised the minimum obtainable temperature to the value stated above.

# CHAPTER V

## RESULTS

After completing the runs on each crystal, graphs were made of the Hall potential versus the magnetic field. For each specimen there were two of these raw data curves, one for each field direction, and they were plotted on the same scale. Fig. 11 shows these curves for the crystal Be-1. If one of the two curves represents V(H) vs. H then the other must be -V(-H) vs. -H. The height of the upper curve at any point is the sum of the Hall potential and the IR drop on the Hall probes, whereas the lower curve is the difference between the Hall potential and the IR drop. This, of course, is due to the fact that reversing the magnetic field through the sample reverses the Hall potential polarity while leaving the IR drop polarity unchanged. It is easy to see that the IR drop equals half the magnitude of the separation between the two curves and that the actual Hall potential at any field equals the average of the curves at that field, that is

$$V = \frac{1}{2}\left[V(H) - V(-H)\right] \tag{14}$$

This quantity is the $V_x$ occurring in Eq. 4 of Chap. 1. With this and the other three quantities --- field strength, H, sample current, I, and sample thickness, t --- the coeffi-

Fig. 11 $V_H$ - H Curves of Be-1

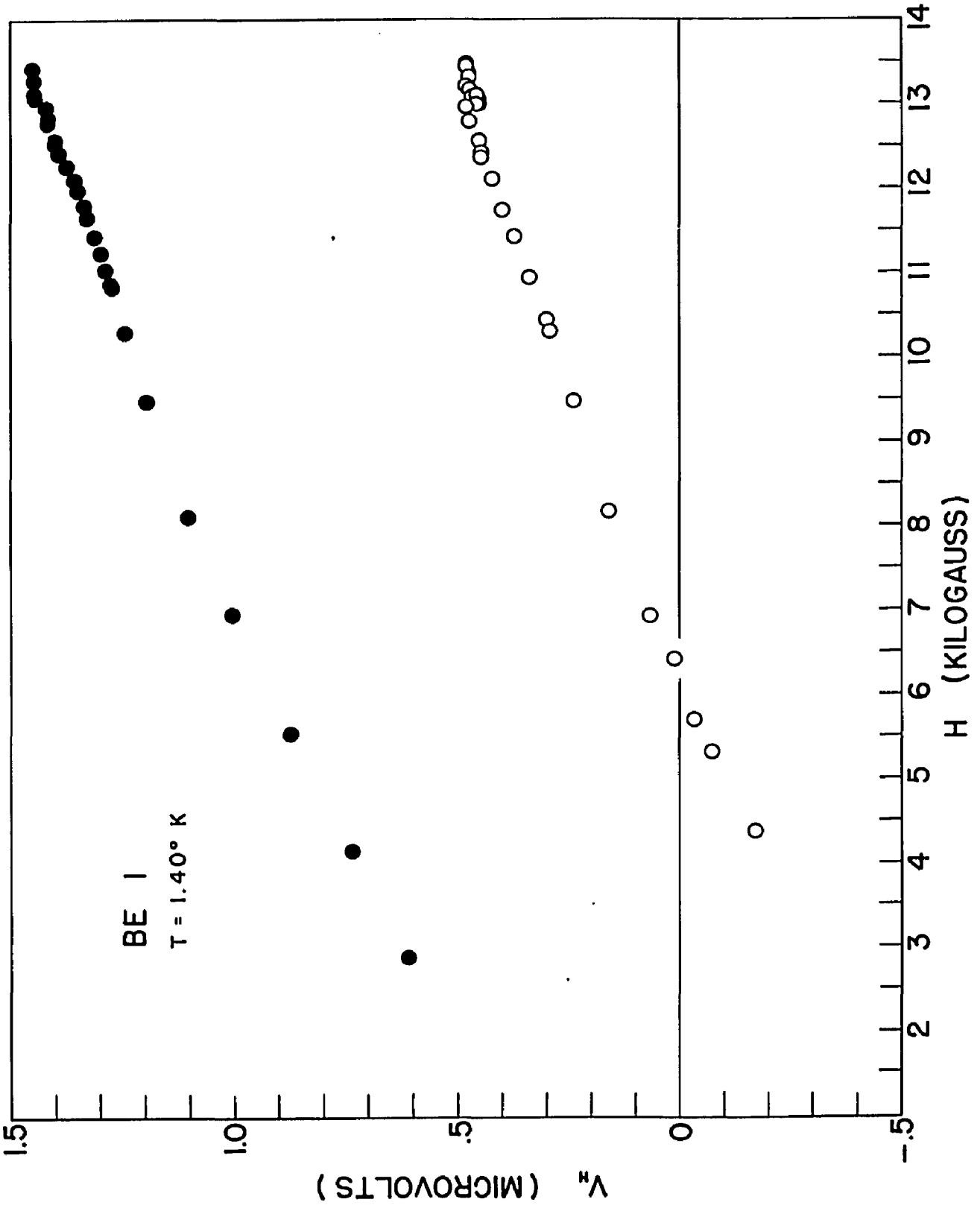

cient R can be evaluated, provided I remains constant or very nearly so throughout both parts of a run.

In Borovik's work cited earlier he explains the shortcomings of the quantity R in the following way. R is ordinarily defined by the relation

$$R = \frac{E_x}{H j_y} \tag{15}$$

where $E_x$ is the Hall field, H the magnetic field, and $j_y$ the current density (perpendicular to both $E_x$ and H). Let $r_H$ and $r_o$ be the resistances in the direction of current in the presence of field H and in zero field respectively; and let $c_H$ and $c_o$ be the corresponding conductances. Then since $j_y = c_H E_x$, Eq. 15 can be written as

$$R = \frac{E_x}{c_H E_y H} = \frac{E_x r_H}{E_y H} = \frac{E_x}{E_y H c_o} \cdot \frac{r_H}{r_o} \tag{16}$$

It is seen from this how R is a partial function of the magnetoresistance $r_H$ and hence is influenced by it as well as the Hall process. For the situations where $r_H/r_o = 1$ only, that is, no field dependent component of resistance, does R become a satisfactory index of the Hall effect. It must be remembered that for most cases this requirement does in fact obtain; it is only at very low temperatures and for certain metals (notably bismuth) that it does not. One could define a Hall coefficient which would be independent of $r_H$ by dividing it out of Eq. 16. Borovik goes a step further and divides out the fraction $r_H/H$ leaving the ratio $E_x/E_y$.

Following his ideas in this work a similar coefficient, to be designated $Q_H$, was defined which eliminated the magnetoresistive term but retained the magnetic field term. It is defined as

$$Q_H = \frac{E_x}{E_y H} \cdot \frac{w}{d} \tag{17}$$

where w and d are constants, w being the width of the sample or lateral distance between Hall probes and d being the vertical displacement or misalignment of the probes. The reason for including the factor w/d is a practical one which becomes apparent when one considers that $wE_x$ and $dE_y$ are the Hall potential and IR drop respectively on the Hall probes. Thus Eq. 17 can be written

$$Q_H = \frac{V_x}{V_{IR} H} = \frac{\frac{1}{2}\left[V(H) - V(-H)\right]}{\frac{1}{2}\left[V(H) + V(-H)\right] H} = \frac{V(H) - V(-H)}{\left[V(H) + V(-H)\right] H} \tag{18}$$

$Q_H$ can be evaluated for any magnetic field by measuring the sum and the difference of the two ordinates of the $V_H$ - H curves at that field value. It is not necessary to know the specimen current or any of the specimen dimensions as is required in calculating R. However, this definition is formulated on the assumption that the current does not vary appreciably during a given run, a condition that was fulfilled in this research. It is important to note that the definition of $Q_H$ becomes meaningless as the difference between the two raw data curves approaches zero, that is,

as the IR drop approaches zero. This could only be realized by obtaining perfect probe alignment, which is nearly impossible to achieve in practice. Nevertheless, it is possible, as happened on two of the beryllium runs, for the $V_H$ - H curves to lie close together due to excellent probe alignment and actually intersect at several portions due to the experimental error spread of the points. In such cases one is compelled to abandon the coefficient $Q_H$ and use one of the others. With the present arrangement of apparatus the author was unable to evaluate Borovik's ratio $E_x/E_y$, so the ordinary Hall coefficient R was employed for the exceptional cases cited above.

After the raw data graphs shown in Figs. 11, 13, 15, 17 and 19 were plotted the best fitting smooth curves were drawn through the points (not shown in these figures). Then the upper and lower ordinates, V(H) and -V(-H), at equally spaced intervals of H were recorded for the entire range of H. The intervals taken were different for different graphs, the smallest being 100 gauss on the Be-3 curves and the largest 200 gauss on the Be-2 curves. $Q_H$ was then computed for each H by the relation

$$Q_H = \frac{\text{Sum Of Ordinates}}{\text{Diff. Of Ordinates} \times H}$$

which is actually Eq. 18. For the two runs in which $Q_H$ could not be used, each pair of ordinates was averaged together to give the Hall potential V at the various magnetic fields, and these were inserted in the ordinary Hall effect formula (Eq. 4) to give the R's.

Fig. 12 $Q_H$ - 1/H Graph of Be-1

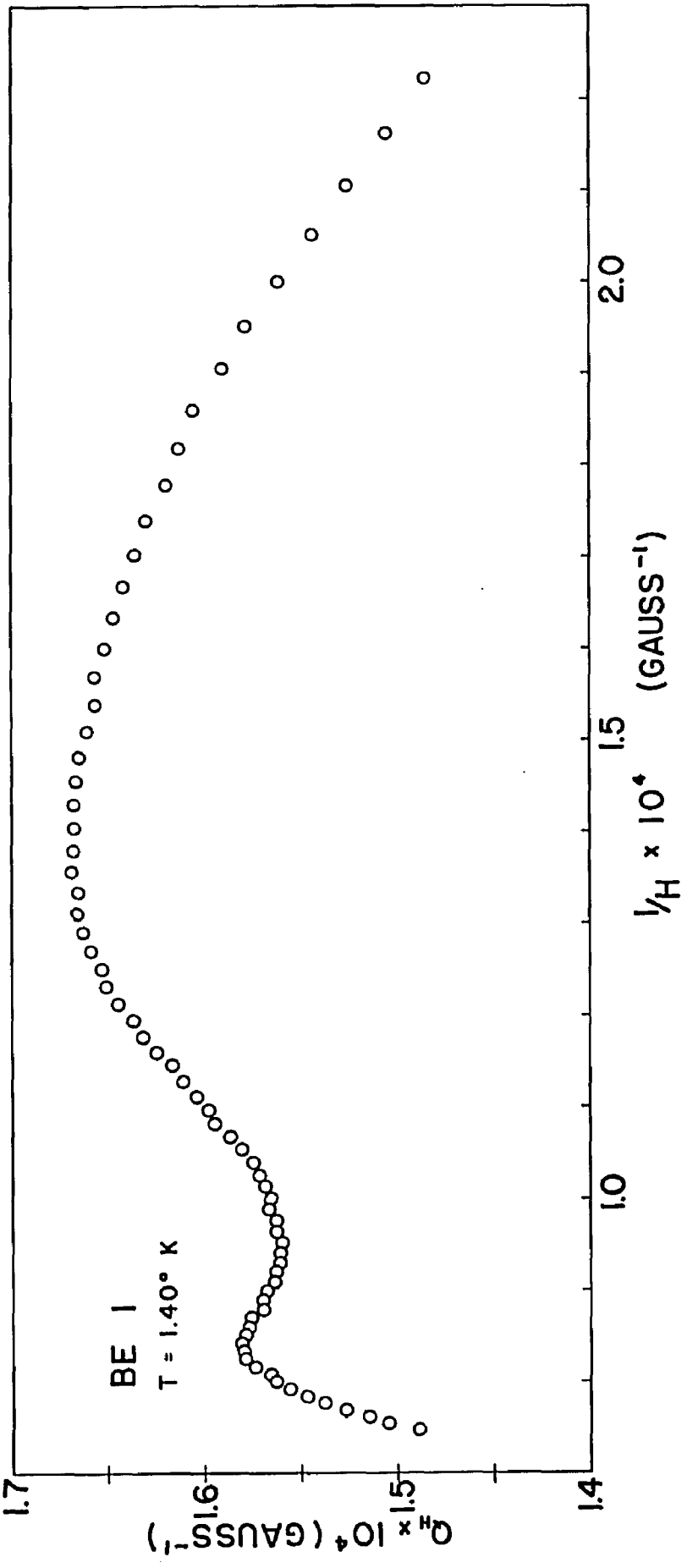

Fig.13 $V_H$ - H Curves of Be-2

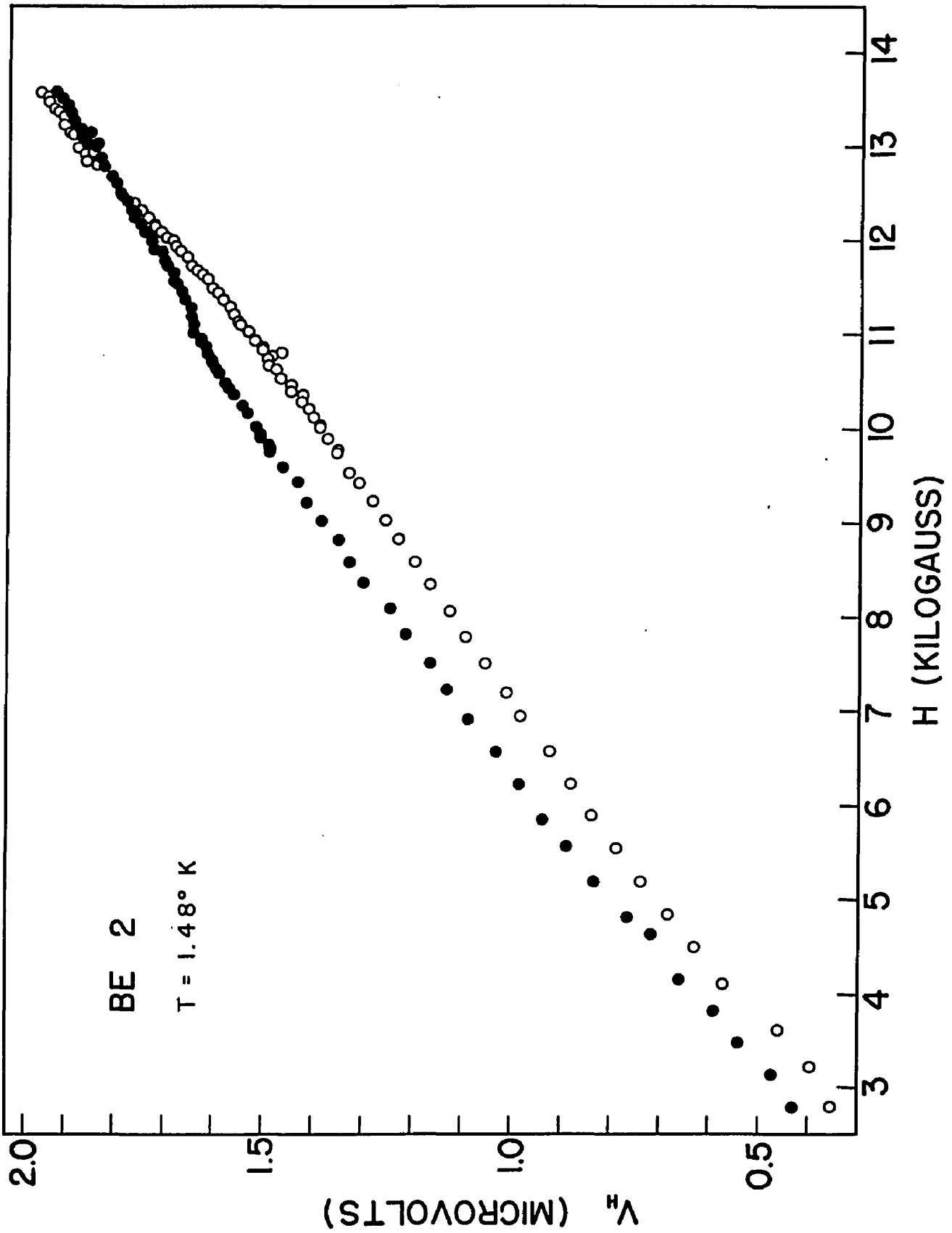

Fig. 14 $R_H$ - 1/H Graph of Be-2

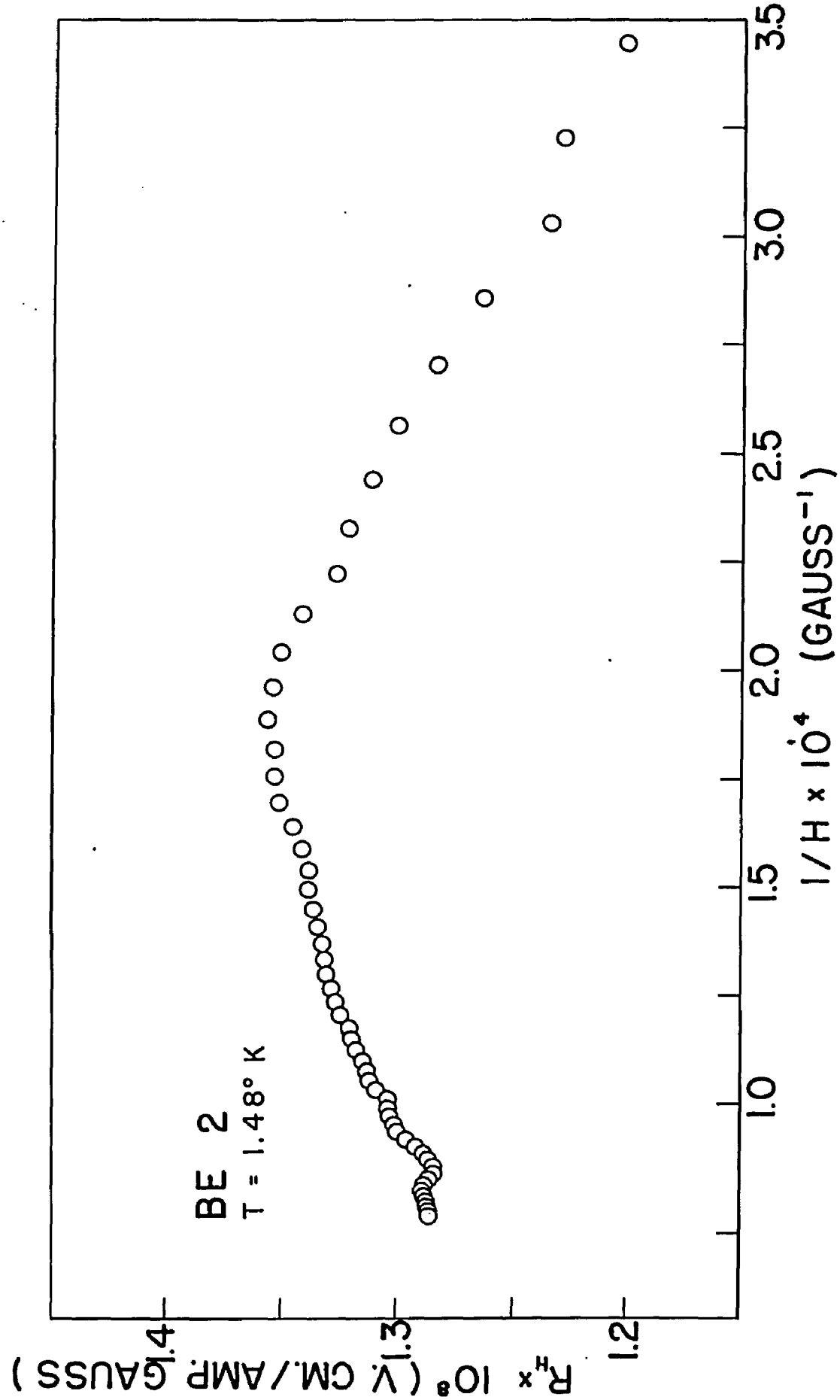

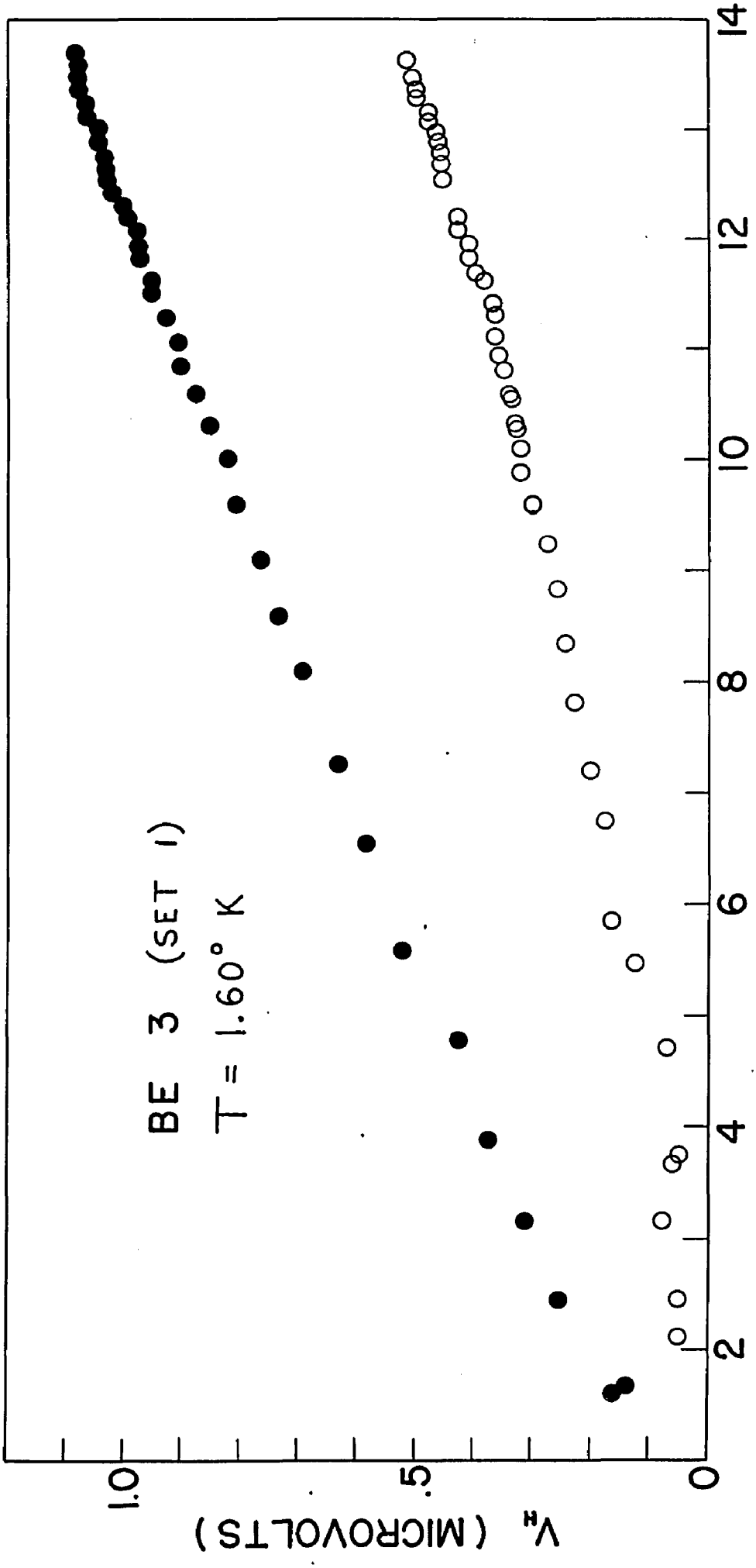


Fig. 15
$V_H$ -H
Curves
of Be-3

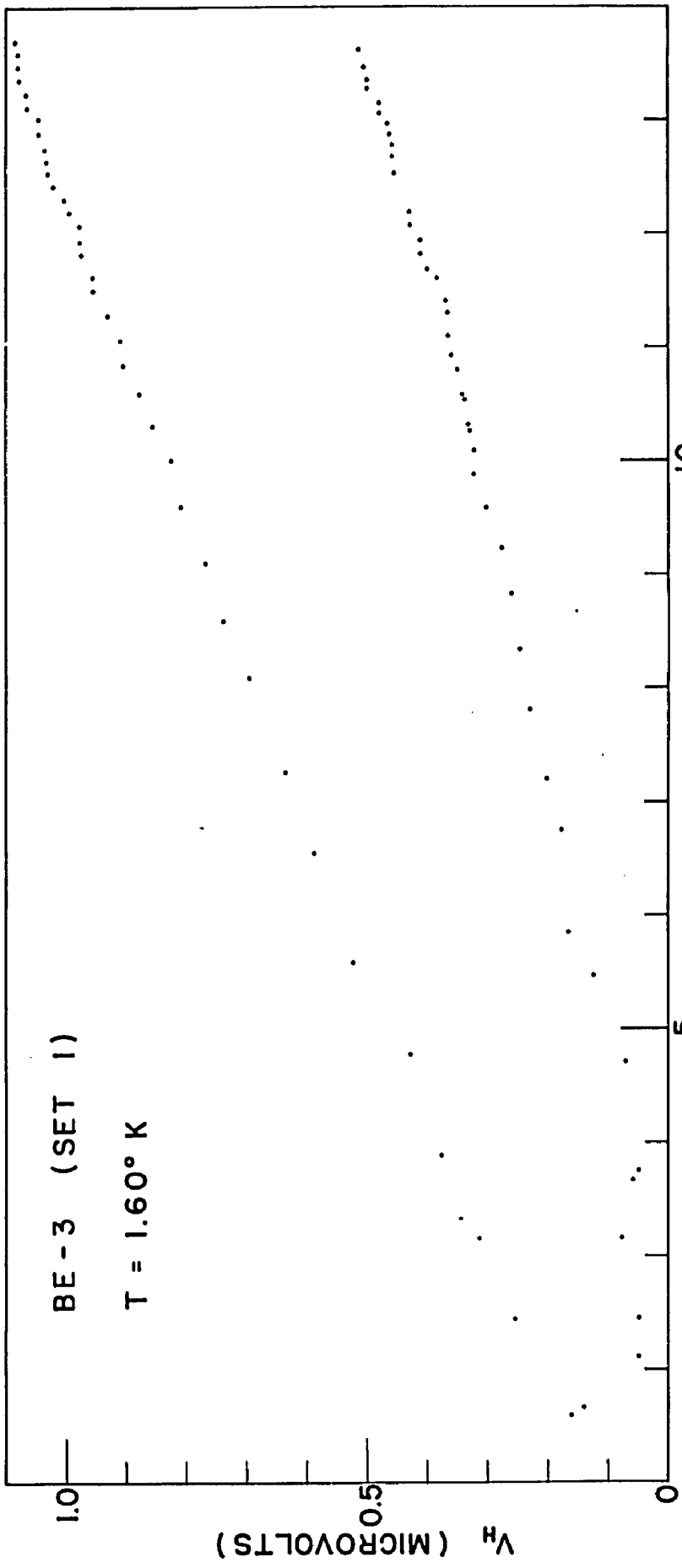


Fig. 15a
Raw Data
Points of
Be-3

Fig. 16 $Q_H$ - 1/H Graph of Be-3

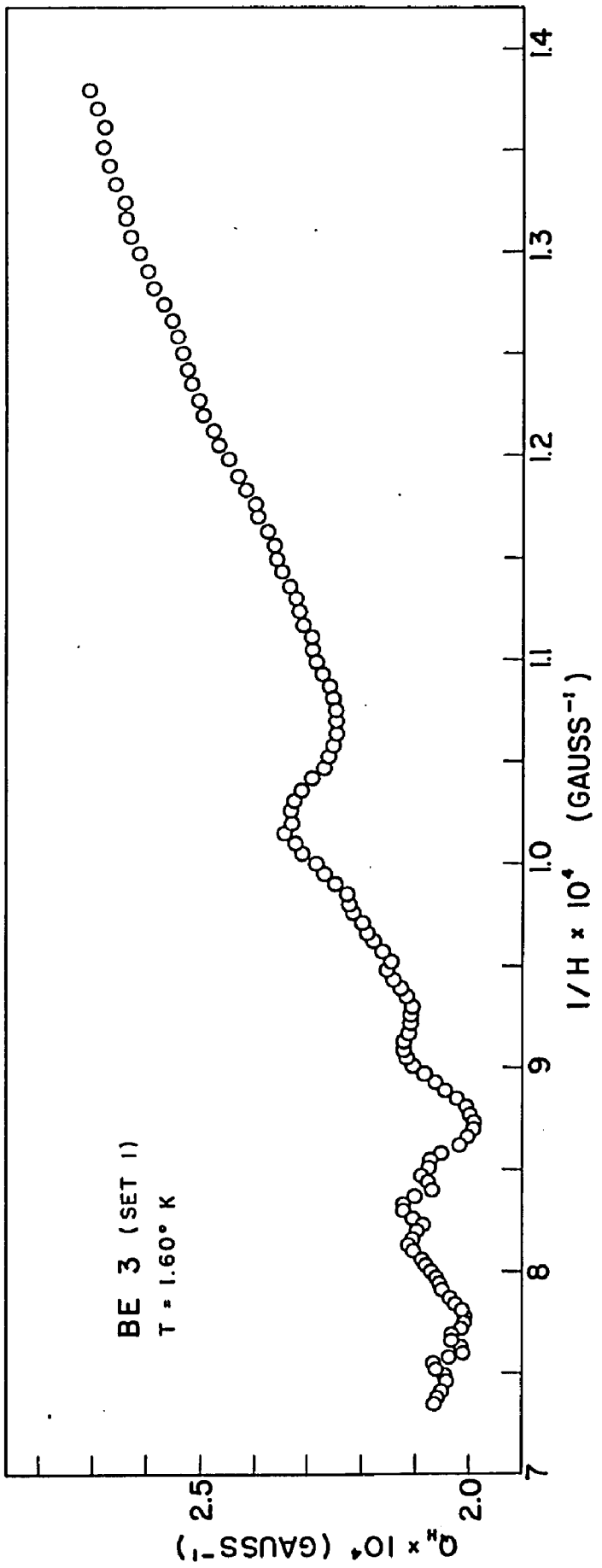

Fig. 17 $V_H$ - H Curves of Be-3

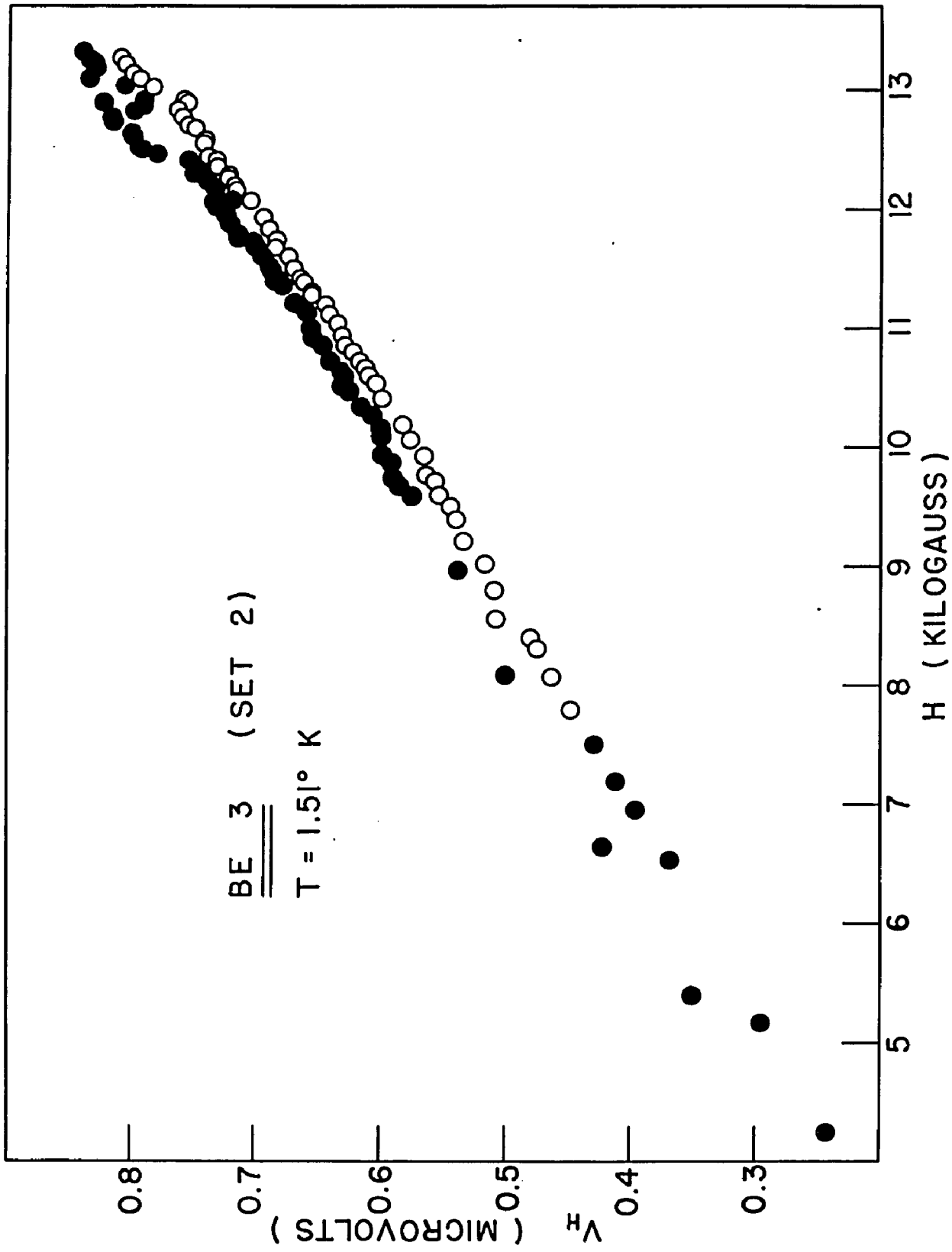

Fig. 18

$R_H$ - 1/H Graph of Be-3

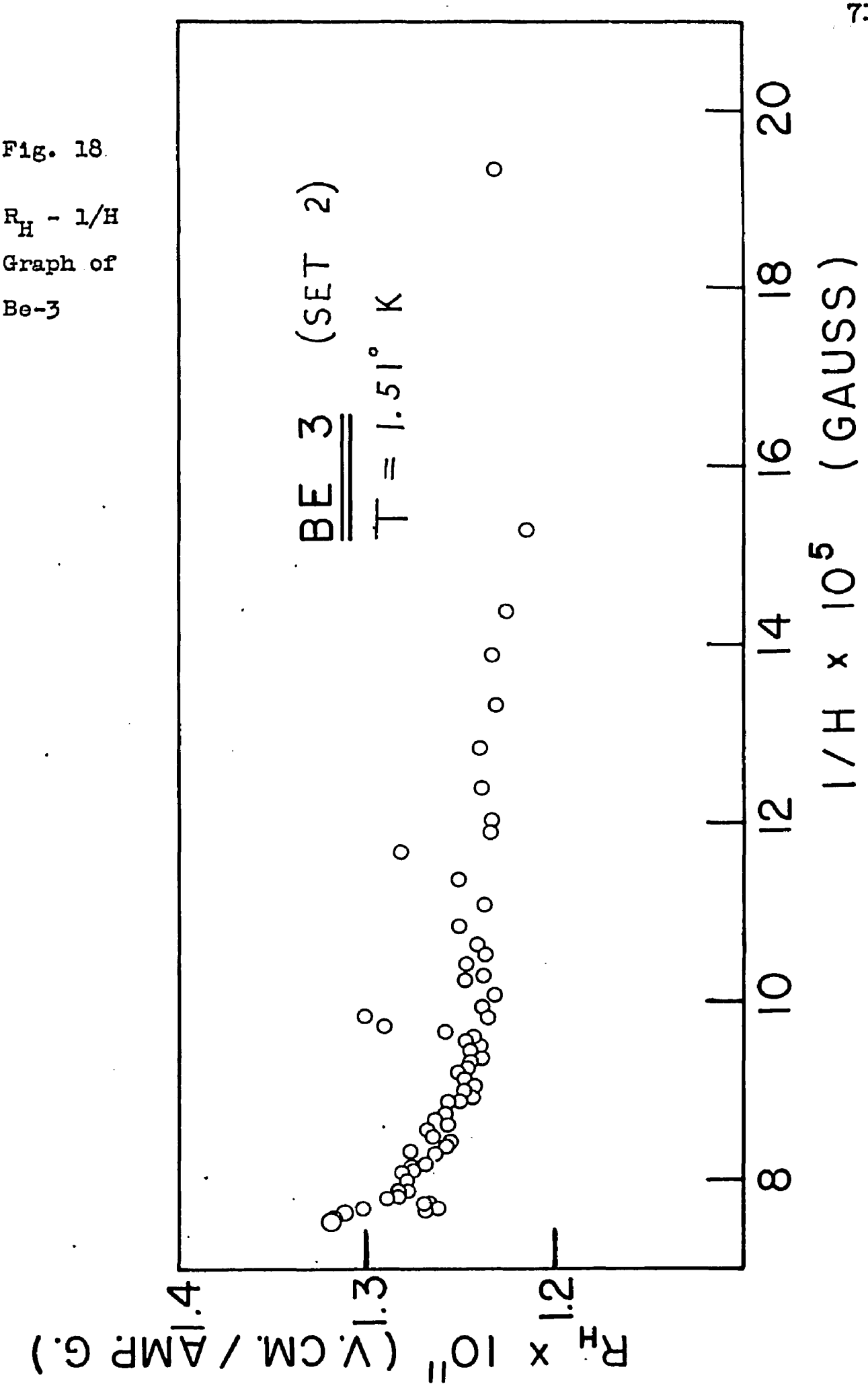

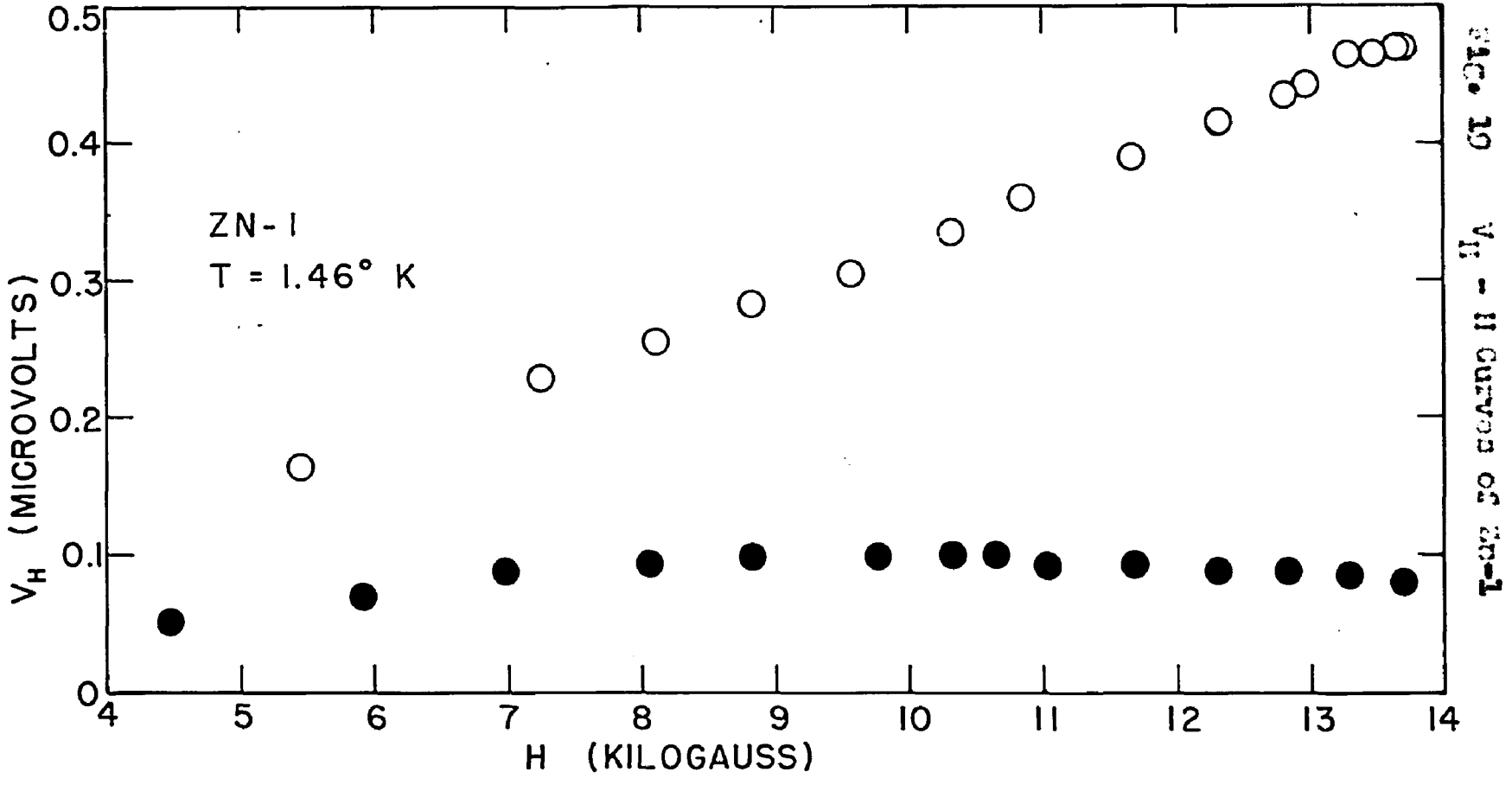
ZN-1
T = 1.46° K
$V_H$ (MICROVOLTS)
H (KILOGAUSS)
0.5
0.4
0.3
0.2
0.1
0
4
5
6
7
8
9
10
11
12
13
14

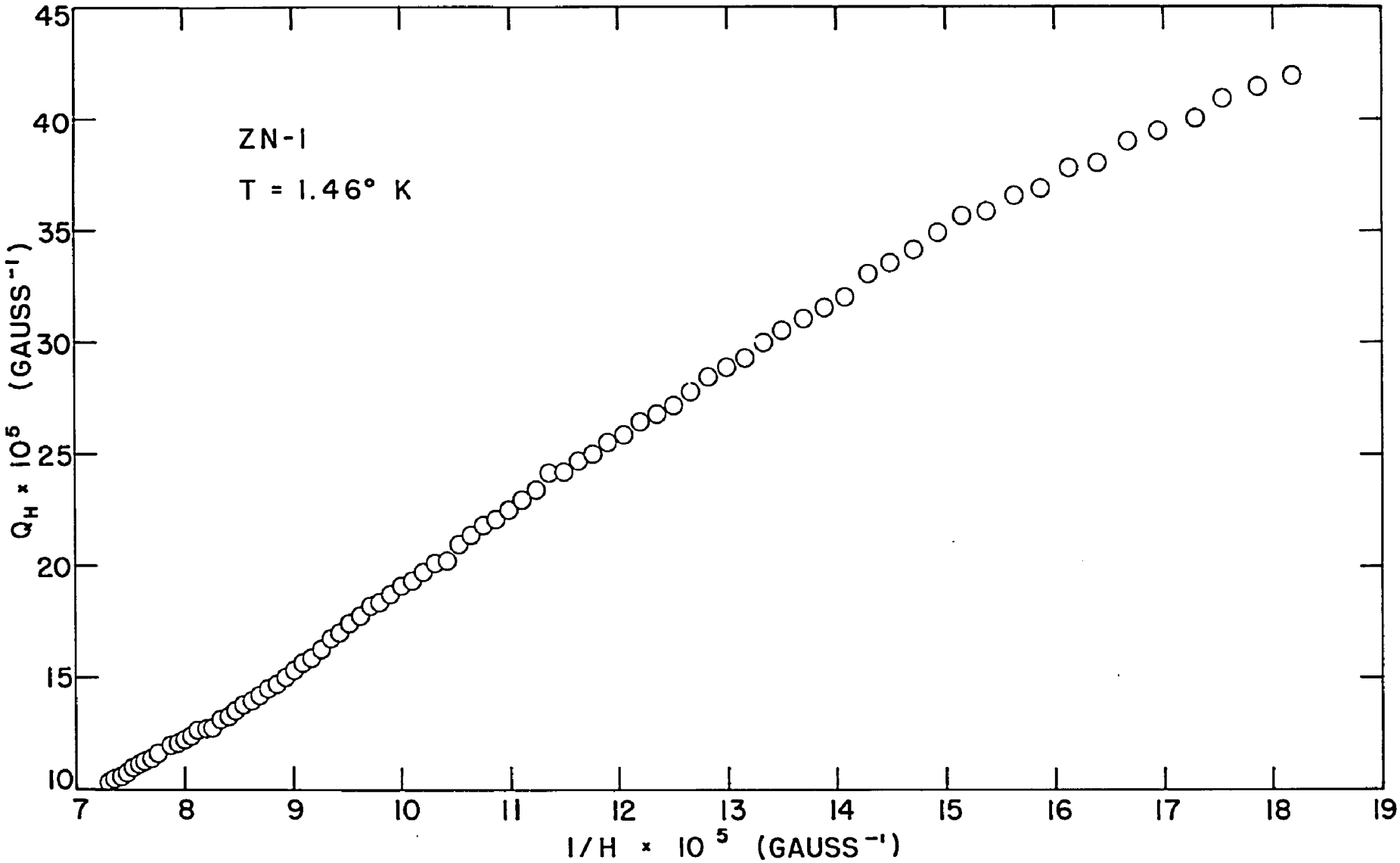


Fig. 20 $Q_H$ - 1/H Graph of Zn-1

Since the field dependent oscillations of the susceptibility, Hall effect, etc., are found to be periodic in the reciprocal of the field it is standard procedure to plot these quantities against 1/H rather than H. In the present work this procedure is followed as a matter of routine, since the primary object was to search for such periodic oscillations.

Figs. 12, 16, and 20 are plots of $Q_H$ vs. 1/H for the sample Be-1, Be-3, and Zn-1 respectively, and Fig. 14 shows R vs. 1/H for the sample Be-2. It can be seen from the raw data plots of Be-2 (Fig. 13) that at high H the curves cross over, making it impossible to calculate $Q_H$. Thus in this case R was calculated and plotted against 1/H. The most interesting graphs are those of Figs. 15 and 16 for Be-3. The pair of $V_H$ - H curves show that $V_H$ rises smoothly for the low and medium fields and then continues upward in step function fashion for the high fields. (Fig. 15). In Fig. 15a, which shows the same curves plotted as points rather than the usual error circles, the step function portions show up more distinctly. Even though the latter point curves represent only approximately the "real" magnitudes, they are presented as an argument for the regularity of the experimental data and to enhance the thesis that the step function is real. The $Q_H$ - 1/H curve of Fig. 16 did not turn out as well as was expected; it goes through small maxima and minima, but not at all in a periodic or regular fashion. A second run was made on this same sample Be-3 to

try and improve the data, however, the results were not as good. Figs. 17 and 18 show the raw and calculated data for this repeat run. The scatter of points, especially at the high fields, is rather bad in both figures.

The total error in the measurement of the Hall potential arose from the following sources: drift of amplifier, drift of working current in potentiometer, background noise in amplifier, and extraneous emf's in Hall circuit. To approximate the magnitude of the amplifier drift the instrument was turned on and allowed to warm up, then the null meter was set at its mid-scale zero position with the dummy circuit on the potentiometer. The instruments were left on for several hours. At the end of such time it was found that the meter had drifted off zero at the rate of about 5 divisions per hour, which was equivalent to an unbalance in the potentiometer of 0.01 microvolts per hour. A part of this unbalance was probably due also to a drift in the working current, hence, both effects should be considered together. A better evaluation of the error from these two sources was made during the course of a run. The meter was zeroed and the potentiometer calibrated twice in each run, once at the beginning of the first field sweep, and once at the beginning of the second field sweep. At the time of the second calibration, 45 min. to an hour after the first, it was noted that the null meter was off zero by an amount equivalent to 0.01 or at most 0.02 microvolts.

This was taken as the combined cumulative error of both drifts.

At low to medium fields the extraneous emf's were extremely small, certainly less than 0.005 microvolts; however, at the high fields they became troublesome and apparently got progressively worse with increasing field. They appeared as slowly varying emf's that oscillated in time with a regular period. The maximum amplitude of these periods was approximately 0.015 microvolts. It is supposed that they were caused by the failure of the compensating loop to check induced emf's from the slight variation of the magnetic field. Since this effect was not noticeable at the lower fields it is presumed that the stray flux outside the poles which activated the loop did not increase in proportion with the main flux through the crystal; so that the correct setting of the loop at low fields was incorrect at the high fields. This slowed the taking of data considerably, since the null meter varied constantly. The best that could be done to offset this was to read the potentiometer by the mean position of the null meter needle.

The background noise of the amplifier need hardly be considered since its effect on accuracy was negligible in comparison with the above mentioned sources of error.

In plotting the raw data curves, $V_H$ - H, the diameters of the circles were taken as the estimated total error in the measurement of the Hall potential but not, as the

curves indicate, as the error in H. The error in field is in fact much smaller than these diameters, being between 100 and 150 gauss. At the low fields the error in $V_H$ is much smaller than indicated; whereas, at the extreme high fields it is perhaps slightly higher. The size of the circles in the other graphs, $Q_H$ - 1/H and R -1/H, are not meant to have any significance since their points were calculated from points on best fitting curves drawn through the raw data circles.

Borovik performed his beryllium Hall measurements on a flat rectangular specimen whose hexagonal axis was perpendicular to the face of the rectangle and hence parallel to the magnetic field. This was equivalent to the sample Be-1 in the present work, although its minor axes were oriented differently. One of the secondary axes (a-axis) of Borovik's sample was 20° off from the direction of the sample current, whereas, the a-axis of Be-1 was parallel to the direction of current. The temperature of his sample during the measurements was 2.14°K as compared with 1.40°K for Be-1. Borovik presents a graph of $E_x/E_y$ vs. H which was replotted in the following way: each $E_x/E_y$ value was divided by its particular H and then plotted against 1/H. The function $E_x/E_yH$ differs from $Q_H$ only by a constant factor since $Q_H = E_x/E_yH$ w/d, hence a relative comparison can be made. This replotted graph is shown in Fig. 21. As can be seen, there is a vast difference between it and the Be-1 curve of Fig. 12. It is hardly possible that the

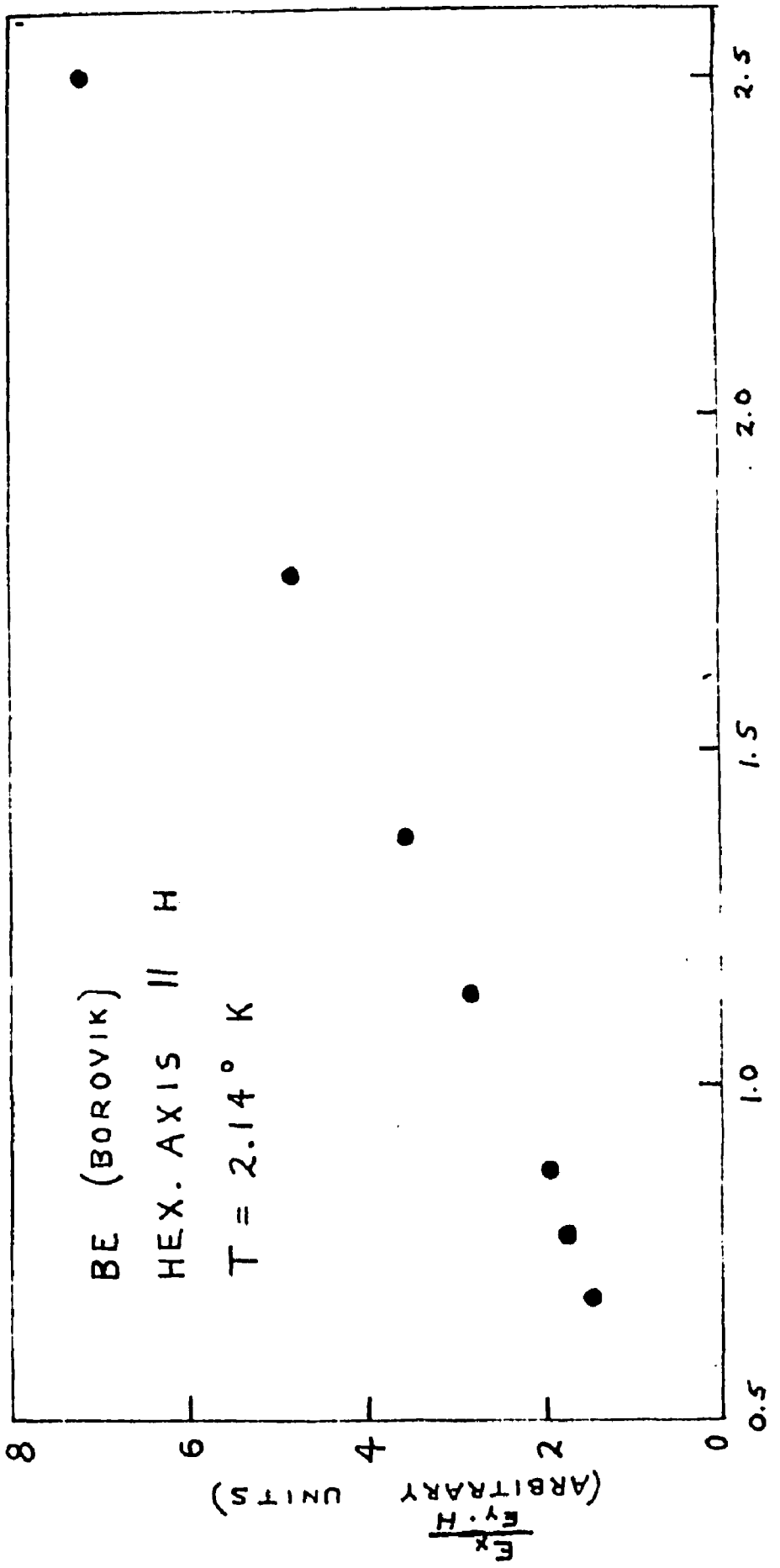


Fig. 21
Borovik's
Results on
Be (Replotted)

temperature difference of 0.74° would account for this contrast. If it is real, it seems that one must look for an explanation either in the slight difference of orientation which is known to have marked effect on the magneto-electric properties of crystals, or perhaps in the difference in purities of the two samples, which is also an influential factor.

The zinc crystal investigated by Borovik was also in the shape of a flat rectangle. Its hexagonal axis made an angle of 14° with the direction of the magnetic field and the Hall meausrements were done at 4.22°K. The zinc sample Zn-1 in the present research had its hexagonal axis oriented 24° relative to the field and its measurements were made at a temperature of 1.46° K. Borovik's zinc data was re-plotted exactly as was done for beryllium and the graph is shown in Fig. 22. A comparison with the Zn-1 graph of Fig. 20 shows the similarity of the two. Both are apparently straight lines, though with different slopes. However, the data were taken on the two samples at the temperatures differing by 2.76° K, and the hexagonal axis of Zn-1 is skewed 10° further from the direction of the magnetic field.

The results of this investigation on the low temperature Hall effect of beryllium crystals at the several orientations reveal no periodic field dependent oscillations as was hoped for. However, the rather erratic oscillations observed in Be-3, despite their borderline character, seem encouraging as a preliminary step. If the oscillations are

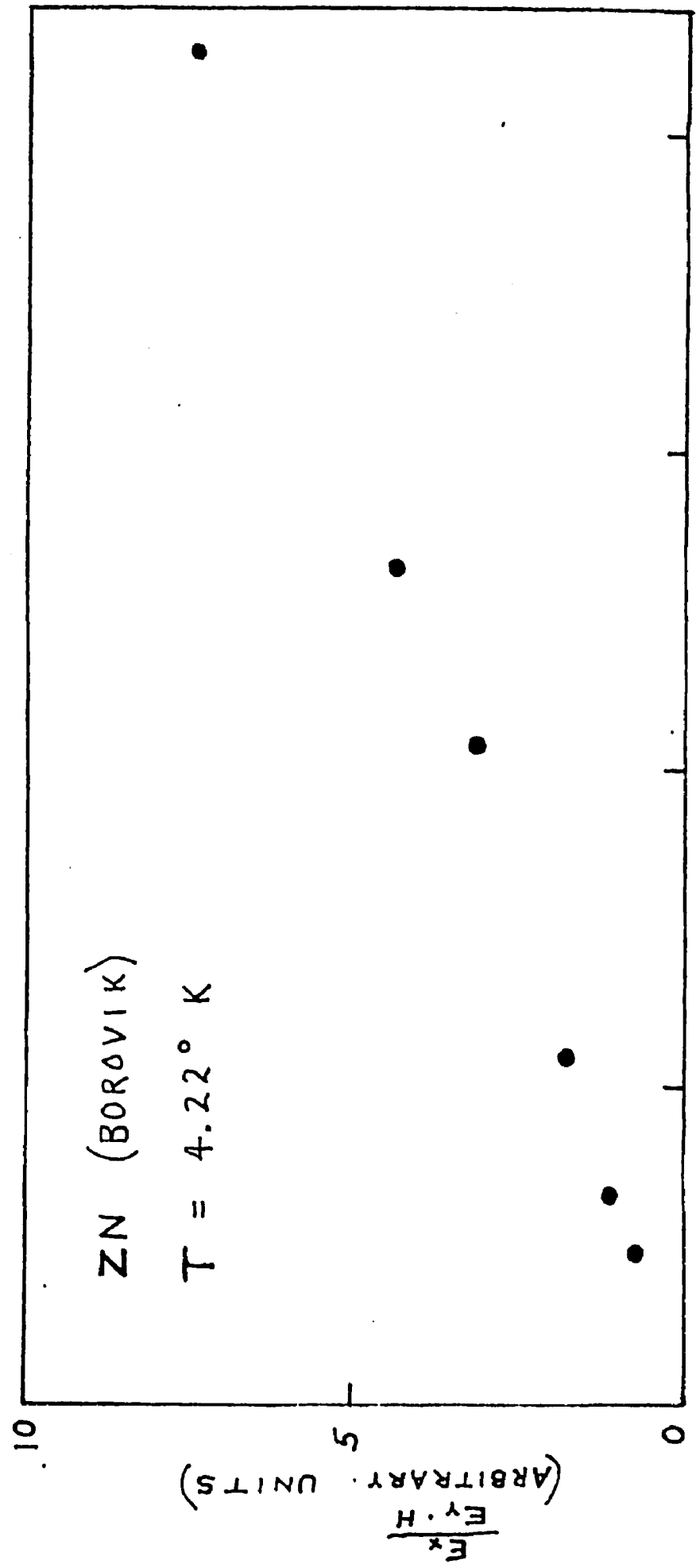


Fig. 22
Borovik's
Results on
Zn (Replotted)

real, lower temperatures and purer crystals should ferret them out. The experiences with the effect in bismuth in this laboratory have shown that a difference in temperature of only a fraction of a degree in the liquid helium range makes a remarkable difference in the amplitudes of the oscillations. For future research another avenue of approach is the obvious one of increasing the measuring sensitivity, but this might not prove as fruitful nor as simple as, say, amplifying the Hall potentials in the crystals themselves by using thinner samples. In such hard metals as beryllium it should not be too difficult to decrease the thickness used here by 5 fold or more. This of course introduces the fresh problem of making adequate and sturdy contact between crystal and probes.

In the case of further investigation in zinc it is apparent that the first need is for measurement on several single crystals of different regular orientations of the crystallographic axes relative to the field and current directions.

## SELECTED BIBLIOGRAPHY


1. F. Bloch, Z. Physik 52, 555 (1928).
2. J. M. Reynolds, T. E. Leinhardt, and H. W. Hemstreet, Phys. Rev. 93, 247 (1954).
3. J. M. Reynolds, H. W. Hemstreet, and T. E. Leinhardt, Phys. Rev. 96, 1203 (1954).
4. T. B. Berlincourt, Phys Rev. 94, 1172 (1954).
5. M. C. Steele, Phys. Rev. 98, 1180(A) (1955).
6. W. J. de Haas and P. M. van Alphen, Leiden Comm. No. 212a (1930) and No. 220d (1932).
7. R. Peierls, Z. Physik 80, 763, (1933).
8. M. Blackman, Proc. Roy. Soc. (London) A166, 1 (1938).
9. L. D. Landau, by private communication to D. Shoenberg. [See Appendix to D. Shoenberg, Proc. Roy. Soc. (London) A170, 341 (1939)].
10. J. A. Marcus, Phys. Rev. 71, 559 (1947).
11. D. Shoenberg, Trans. Roy. Soc. (London) A245, 1 (1952).
12. T. G. Berlincourt and J. K. Logan, Phys. Rev. 93, 348 (1954); also T. G. Berlincourt, Phys. Rev. 91, 1277 (1953).
13. P. B. Alers and R. T. Webber, Phys. Rev. 91, 1060 (1953).
14. A. H. Gerritsen and W. J. de Haas, Leiden Comm. 216b (1940).

15 R. A. Connell and J. A. Marcus, National Science Foundation Conference on Low Temperature Physics and Chemistry (1955).

16. M. C. Steele and J. Babiskin, Phys. Rev. 94, 1394 (1954).

17. J. Babiskin and M. C. Steele, Bull. Am. Phys. Soc. 29, 11 (1954).

18. J. S. Levinger and E. G. Grimsal, Phys. Rev. 94, 772(A) (1954).

19. R. B. Dingle, Proc. Roy. Soc. (London) A211, 500 (1952).

20. E. S. Borovik, Doklady Acad. Nauk S. S. S. R. 70, 601 (1950); and J. Exptl. Theoret. Phys. (U. S. S. R.) 23, 83 (1953).

21. P. W. Bridgman, Proc. Am. Acad. Arts Sciences 60, 303 (1925).

# APPENDIX

## Table II

### Be-1 Raw Data (T = 1.40° K)

| V(H) (microvolts) | H (gauss) | -V(-H) (microvolts) | -H (gauss) |
|---|---|---|---|
| 0.61 | 2875 | -0.168 | 4370 |
| 0.735 | 4135 | -0.071 | 5310 |
| 0.873 | 5525 | -0.030 | 5695 |
| 1.005 | 6940 | 0.014 | 6410 |
| 1.103 | 8100 | 0.069 | 6925 |
| 1.195 | 9470 | 0.161 | 8160 |
| 1.244 | 10290 | 0.240 | 9475 |
| 1.273 | 10815 | 0.293 | 10300 |
| 1.275 | 10860 | 0.300 | 10440 |
| 1.288 | 11030 | 0.337 | 10940 |
| 1.298 | 11230 | 0.371 | 11425 |
| 1.311 | 11425 | 0.399 | 11740 |
| 1.329 | 11650 | 0.420 | 12105 |
| 1.337 | 11790 | 0.446 | 12365 |
| 1.350 | 11975 | 0.446 | 12425 |
| 1.357 | 12105 | 0.451 | 12560 |
| 1.374 | 12265 | 0.473 | 12785 |
| 1.392 | 12420 | 0.481 | 12960 |
| 1.400 | 12530 | 0.466 | 12990 |
| 1.400 | 12560 | 0.457 | 12995 |
| 1.399 | 12570 | 0.451 | 13000 |
| 1.494 | 12610 | 0.451 | 13045 |
| 1.405 | 12655 | 0.466 | 13075 |
| 1.417 | 12775 | 0.456 | 13105 |
| 1.416 | 12835 | 0.475 | 13125 |
| 1.420 | 12955 | 0.465 | 13155 |
| 1.446 | 13080 | 0.472 | 13165 |
| 1.447 | 13120 | 0.482 | 13210 |
| 1.432 | 13145 | 0.480 | 13215 |
| 1.447 | 13165 | 0.481 | 13230 |
| 1.445 | 13210 | 0.468 | 13250 |
| 1.448 | 13280 | 0.475 | 13285 |
| 1.450 | 13415 | 0.475 | 13320 |
| | | 0.475 | 13360 |
| | | 0.480 | 13395 |
| | | 0.480 | 13440 |
| | | 0.480 | 13475 |
| | | 0.488 | 13545 |
| | | 0.488 | 13575 |
| | | 0.488 | 13610 |

Table III

Be-2 Raw Data (T = 1.48° K)

| V(H) (microvolts) | H (gauss) | V(H) (microvolts) | H (gauss) | V(H) (microvolts) | H (gauss) |
|---|---|---|---|---|---|
| .353 | 2800 | 1.529 | 10980 | 1.790 | 12515 |
| .395 | 3225 | 1.535 | 11025 | 1.794 | 12530 |
| .460 | 3620 | 1.542 | 11050 | 1.802 | 12565 |
| .573 | 4110 | 1.550 | 11100 | 1.802 | 12575 |
| .630 | 4500 | 1.554 | 11130 | 1.802 | 12600 |
| .682 | 4850 | 1.564 | 11205 | 1.812 | 12635 |
| .738 | 5200 | 1.573 | 11245 | 1.812 | 12670 |
| .788 | 5550 | 1.571 | 11290 | 1.820 | 12690 |
| .839 | 5900 | 1.582 | 11310 | 1.826 | 12730 |
| .880 | 6230 | 1.585 | 11360 | 1.826 | 12755 |
| .922 | 6575 | 1.593 | 11400 | 1.836 | 12775 |
| .982 | 6950 | 1.606 | 11485 | 1.842 | 12790 |
| 1.010 | 7200 | 1.610 | 11540 | 1.842 | 12815 |
| 1.053 | 7510 | 1.617 | 11580 | 1.864 | 12835 |
| 1.093 | 7790 | 1.627 | 11625 | 1.847 | 12870 |
| 1.126 | 8065 | 1.639 | 11675 | 1.866 | 12915 |
| 1.165 | 8345 | 1.649 | 11720 | 1.850 | 12925 |
| 1.198 | 8590 | 1.650 | 11755 | 1.860 | 12950 |
| 1.230 | 8830 | 1.651 | 11770 | 1.880 | 12975 |
| 1.257 | 9030 | 1.651 | 11780 | 1.871 | 12995 |
| 1.282 | 9235 | 1.659 | 11810 | 1.888 | 13020 |
| 1.309 | 9420 | 1.658 | 11820 | 1.876 | 13060 |
| 1.330 | 9530 | 1.670 | 11830 | 1.886 | 13100 |
| 1.355 | 9740 | 1.667 | 11850 | 1.890 | 12120 |
| 1.352 | 9770 | 1.672 | 11875 | 1.896 | 13140 |
| 1.362 | 9785 | 1.679 | 11910 | 1.896 | 13155 |
| 1.373 | 9890 | 1.681 | 11930 | 1.904 | 13180 |
| 1.388 | 10010 | 1.686 | 11990 | 1.904 | 13195 |
| 1.389 | 10035 | 1.700 | 12020 | 1.910 | 13225 |
| 1.395 | 10075 | 1.710 | 12065 | 1.901 | 12250 |
| 1.402 | 10120 | 1.710 | 12080 | 1.909 | 13310 |
| 1.411 | 10205 | 1.714 | 12115 | 1.920 | 13360 |
| 1.425 | 10280 | 1.724 | 12140 | 1.929 | 13370 |
| 1.423 | 10355 | 1.724 | 12160 | 1.929 | 13400 |
| 1.447 | 10390 | 1.724 | 12190 | 1.940 | 13465 |
| 1.447 | 10460 | 1.734 | 12215 | 1.940 | 13520 |
| 1.468 | 10535 | 1.738 | 12235 | 1.955 | 13565 |
| 1.478 | 10620 | 1.742 | 12260 | | |
| 1.493 | 10670 | 1.752 | 12290 | | |
| 1.495 | 10735 | 1.752 | 12310 | | |
| 1.487 | 10775 | 1.757 | 12335 | | |
| 1.466 | 10805 | 1.764 | 12360 | | |
| 1.506 | 10830 | 1.766 | 12385 | | |
| 1.506 | 10865 | 1.773 | 12415 | | |
| 1.506 | 10875 | 1.773 | 12460 | | |
| 1.515 | 10900 | 1.790 | 12470 | | |
| 1.521 | 10930 | 1.785 | 12490 | | |

Table III (con't.)

| -V(-H) (microvolts) | -H (gauss) | -V(-H) (microvolts) | -H (gauss) | -V(-H) (microvolts) | -H (gauss) |
|---|---|---|---|---|---|
| .430 | 2800 | 1.623 | 10875 | 1.800 | 12550 |
| .473 | 3150 | 1.625 | 10910 | 1.805 | 12585 |
| .541 | 3485 | 1.630 | 10920 | 1.805 | 12605 |
| .590 | 3825 | 1.630 | 10950 | 1.811 | 12635 |
| .661 | 4160 | 1.933 | 10975 | 1.817 | 12675 |
| .717 | 4640 | 1.646 | 11015 | 1.825 | 12710 |
| .764 | 4820 | 1.640 | 11060 | 1.818 | 12735 |
| .832 | 5200 | 1.645 | 11100 | 1.828 | 12755 |
| .888 | 5575 | 1.645 | 11115 | 1.828 | 12780 |
| .936 | 5850 | 1.645 | 11150 | 1.828 | 12810 |
| .983 | 6230 | 1.650 | 11185 | 1.830 | 12830 |
| 1.030 | 6570 | 1.650 | 11220 | 1.835 | 12875 |
| 1.087 | 6920 | 1.650 | 11275 | 1.838 | 12920 |
| 1.130 | 7235 | 1.656 | 11305 | 1.845 | 12990 |
| 1.165 | 7510 | 1.662 | 11365 | 1.840 | 13015 |
| 1.215 | 7820 | 1.668 | 11405 | 1.862 | 13020 |
| 1.245 | 8090 | 1.670 | 11450 | 1.862 | 13055 |
| 1.300 | 8365 | 1.680 | 11500 | 1.873 | 13100 |
| 1.328 | 8585 | 1.679 | 11530 | 1.855 | 13140 |
| 1.350 | 8820 | 1.685 | 11560 | 1.875 | 13150 |
| 1.385 | 9020 | 1.685 | 11605 | 1.876 | 13175 |
| 1.415 | 9215 | 1.685 | 11650 | 1.884 | 13220 |
| 1.432 | 9425 | 1.696 | 11675 | 1.888 | 13255 |
| 1.463 | 9590 | 1.699 | 11725 | 1.876 | 13270 |
| 1.490 | 9755 | 1.705 | 11750 | 1.882 | 13310 |
| 1.488 | 9785 | 1.705 | 11785 | 1.895 | 13350 |
| 1.492 | 9825 | 1.710 | 11820 | 1.895 | 13385 |
| 1.492 | 9875 | 1.710 | 11870 | 1.900 | 13425 |
| 1.509 | 9900 | 1.726 | 11895 | 1.900 | 13475 |
| 1.509 | 9940 | 1.733 | 11935 | 1.913 | 13500 |
| 1.517 | 10020 | 1.730 | 11980 | 1.919 | 13540 |
| 1.525 | 10060 | 1.730 | 12010 | 1.925 | 13570 |
| 1.535 | 10160 | 1.739 | 12055 | | |
| 1.545 | 10240 | 1.743 | 12085 | | |
| 1.552 | 10290 | 1.750 | 12135 | | |
| 1.563 | 10355 | 1.752 | 12165 | | |
| 1.573 | 10425 | 1.757 | 12195 | | |
| 1.584 | 10530 | 1.765 | 12240 | | |
| 1.593 | 10585 | 1.765 | 12275 | | |
| 1.600 | 10650 | 1.771 | 12310 | | |
| 1.608 | 10700 | 1.780 | 12360 | | |
| 1.608 | 10725 | 1.780 | 12415 | | |
| 1.614 | 10750 | 1.785 | 12445 | | |
| 1.616 | 10790 | 1.785 | 12460 | | |
| 1.616 | 10800 | 1.791 | 12465 | | |
| 1.623 | 10840 | 1.794 | 12490 | | |
| 1.620 | 10865 | 1.794 | 12515 | | |

Table IV

Be-3 (Set 1) Raw Data (T = 1.60° K)

| V(H) (microvolts) | H (gauss) | -V(-H) (microvolts) | -H (gauss) |
|---|---|---|---|
| .140 | 1675 | .161 | 1600 |
| .050 | 2455 | .254 | 2450 |
| .078 | 3160 | .314 | 3160 |
| .060 | 3670 | .375 | 3890 |
| .050 | 3755 | .428 | 4780 |
| .072 | 4710 | .523 | 5590 |
| .125 | 5470 | .587 | 6545 |
| .166 | 5850 | .635 | 7260 |
| .178 | 6750 | .695 | 8090 |
| .202 | 7200 | .738 | 8590 |
| .230 | 7810 | .768 | 9100 |
| .245 | 8340 | .809 | 9595 |
| .260 | 8825 | .825 | 10005 |
| .276 | 9235 | .856 | 10305 |
| .302 | 9590 | .878 | 10590 |
| .323 | 9880 | .905 | 10840 |
| .323 | 10090 | .910 | 11060 |
| .330 | 10270 | .931 | 11280 |
| .332 | 10320 | .956 | 11500 |
| .338 | 10540 | .956 | 11620 |
| .342 | 10580 | .975 | 11815 |
| .350 | 10800 | .978 | 11930 |
| .360 | 10930 | .978 | 12070 |
| .366 | 11100 | .996 | 12190 |
| .366 | 11300 | 1.004 | 12300 |
| .370 | 11405 | 1.022 | 12420 |
| .385 | 11610 | 1.030 | 12530 |
| .400 | 11685 | 1.033 | 12635 |
| .412 | 11820 | 1.035 | 12740 |
| .412 | 11945 | 1.046 | 12880 |
| .429 | 12075 | 1.046 | 13010 |
| .430 | 12190 | 1.065 | 13105 |
| .455 | 12530 | 1.067 | 13225 |
| .458 | 12675 | 1.078 | 13350 |
| .458 | 12775 | 1.080 | 13465 |
| .463 | 12875 | 1.080 | 13580 |
| .466 | 12965 | 1.085 | 13690 |
| .480 | 13060 | | |
| .480 | 13145 | | |
| .500 | 13275 | | |
| .500 | 13350 | | |
| .506 | 13465 | | |
| .514 | 13620 | | |

Table V

Be-3(Set 2) Raw Data ($T = 1.51^{\circ}K$)

| V(H) (microvolts) | H (gauss) | V(H) (microvolts) | H (gauss) |
|---|---|---|---|
| .186 | 2570 | .731 | 12070 |
| .256 | 3790 | .720 | 12075 |
| .350 | 5400 | .724 | 12100 |
| .422 | 6650 | .725 | 12125 |
| .500 | 8090 | .730 | 12125 |
| .538 | 8975 | .733 | 12140 |
| .575 | 9590 | .733 | 12175 |
| .585 | 9675 | .733 | 12190 |
| .590 | 9740 | .732 | 12200 |
| .592 | 9870 | .738 | 12220 |
| .599 | 9935 | .740 | 12240 |
| .591 | 9875 | .745 | 12275 |
| .600 | 10090 | .751 | 12305 |
| .601 | 10160 | .750 | 12325 |
| .607 | 10270 | .745 | 12325 |
| .616 | 10340 | .751 | 12370 |
| .616 | 10415 | .751 | 12400 |
| .626 | 10470 | .755 | 12405 |
| .630 | 10530 | .755 | 12415 |
| .630 | 10600 | .781 | 12470 |
| .632 | 10635 | .793 | 12510 |
| .641 | 10720 | .795 | 12520 |
| .642 | 10735 | .795 | 12570 |
| .646 | 10790 | .800 | 12615 |
| .647 | 10850 | .799 | 12630 |
| .655 | 10920 | .801 | 12640 |
| .656 | 10995 | .800 | 12720 |
| .660 | 11125 | .816 | 12740 |
| .670 | 11210 | .817 | 12770 |
| .679 | 11355 | .799 | 12825 |
| .685 | 11385 | .792 | 12865 |
| .683 | 11405 | .824 | 12900 |
| .690 | 11515 | .792 | 12925 |
| .693 | 11560 | .791 | 12970 |
| .696 | 11605 | .791 | 13015 |
| .701 | 11685 | .807 | 13040 |
| .703 | 11725 | .800 | 13060 |
| .715 | 11755 | .835 | 13105 |
| .715 | 11790 | .830 | 13190 |
| .716 | 11840 | .831 | 13230 |
| .722 | 11880 | .835 | 13260 |
| .728 | 11915 | .835 | 13290 |
| .724 | 11945 | .840 | 13325 |
| .730 | 11980 | | |
| .730 | 12010 | | |
| .733 | 12020 | | |
| .735 | 12060 | | |

Table V (con't.)

| -V(H) (microvolts) | -H (gauss) | -V(H) (microvolts) | -H (gauss) |
|---|---|---|---|
| .243 | 4250 | .675 | 11540 |
| .295 | 5170 | .675 | 11600 |
| .368 | 6540 | .685 | 11675 |
| .395 | 6960 | .685 | 11745 |
| .411 | 7200 | .690 | 11785 |
| .428 | 7510 | .690 | 11825 |
| .447 | 7790 | .690 | 11880 |
| .463 | 8070 | .695 | 11930 |
| .475 | 8310 | .710 | 12010 |
| .480 | 8400 | .706 | 12070 |
| .508 | 8560 | .711 | 12120 |
| .510 | 8800 | .717 | 12165 |
| .517 | 9015 | .718 | 12200 |
| .534 | 9215 | .724 | 12260 |
| .540 | 9400 | .723 | 12290 |
| .544 | 9500 | .728 | 12325 |
| .554 | 9600 | .733 | 12360 |
| .557 | 9715 | .733 | 12385 |
| .564 | 9770 | .733 | 12415 |
| .566 | 9920 | .738 | 12440 |
| .577 | 10060 | .740 | 12500 |
| .611 | 10140 | .743 | 12550 |
| .583 | 10195 | .743 | 12580 |
| .613 | 10260 | .747 | 12640 |
| .603 | 10355 | .750 | 12680 |
| .599 | 10405 | .755 | 12710 |
| .604 | 10460 | .760 | 12770 |
| .604 | 10530 | .760 | 12790 |
| .610 | 10585 | .765 | 12825 |
| .611 | 10635 | .756 | 12900 |
| .613 | 10670 | .759 | 12920 |
| .618 | 10720 | .760 | 13005 |
| .623 | 10800 | .763 | 13000 |
| .629 | 10855 | .785 | 13020 |
| .632 | 10940 | .795 | 13095 |
| .634 | 10990 | .799 | 13125 |
| .635 | 11040 | .800 | 13155 |
| .642 | 11115 | .806 | 13215 |
| .643 | 11150 | .810 | 13265 |
| .645 | 11200 | | |
| .651 | 11250 | | |
| .656 | 11280 | | |
| .656 | 11305 | | |
| .660 | 11355 | | |
| .662 | 11385 | | |
| .665 | 11420 | | |
| .671 | 11500 | | |

Table VI

Zn-1 Raw Data (T = 1.46° K)

| V(H) (microvolts) | H (gauss) | -V(H) (microvolts) | -H (gauss) |
|---|---|---|---|
| .164 | 5450 | .052 | 4475 |
| .229 | 7250 | .070 | 5915 |
| .256 | 8110 | .088 | 6980 |
| .283 | 8825 | .094 | 8065 |
| .305 | 9575 | .099 | 8830 |
| .335 | 10320 | .099 | 9770 |
| .360 | 10850 | .100 | 10325 |
| .390 | 11670 | .100 | 10650 |
| .415 | 12320 | .092 | 11030 |
| .435 | 12805 | .093 | 11685 |
| .443 | 12970 | .088 | 12385 |
| .465 | 13285 | .088 | 12825 |
| .465 | 13475 | .085 | 13290 |
| .470 | 13650 | .080 | 13695 |
| .470 | 13700 | | |

# V I T A

Harold W. Hemstreet, Jr., was born in New Orleans, Louisiana on November 19, 1927. He attended St. Joseph's Parochial School and Jesuit High School. He was graduated from the latter in May, 1944, and the following October enrolled at Loyola University. In February, 1946, he left this institution and enlisted in the Navy for a period of two years. While in the Navy he attended electronics technician schools for one year and served the remainder of his enlistment as a radio technician aboard ship. After being discharged he re-entered Loyola University in February, 1948, and was graduated with a B. S. in Physics in June, 1950. He enrolled in the Graduate School of Louisiana State University in June, 1950, and received his M. S. degree in physics in June, 1952. He returned to Louisiana State University in September, 1952 to continue graduate studies, and is at present a candidate for the Doctor of Philosophy degree in the Department of Physics.

## EXAMINATION AND THESIS REPORT

Candidate: Harold William Hemstreet, Jr.

Major Field: Physics

Title of Thesis: The Low Temperature Hall Effect in Single Crystals of Beryllium and Zinc

Approved:

J. M. Reynolds
Major Professor and Chairman

Howard L. Hall
Dean of the Graduate School

EXAMINING COMMITTEE:

Vincent E. Parker

Max Goodrich

D E Ralph

E. Schlechter

Date of Examination: July 5, 1956